1.1 Preface

Theoretically-inspired design of chromophores with exceptional molecular first hyperpolarizability and nanoscopically-engineered to control intermolecular electrostatic interactions for enhanced acentric chromophore order has produced dramatic improvements in electro-optic activity to values more than 15 times the best inorganic material, crystalline lithium niobate. The large electro-optic coefficients of solution-processed organic electro-optic materials permit drive voltages in devices to be reduced to values of less than 1 volt. Such voltages are critical to the realization of gain in radiofrequency-microwave-millimeter/photonic applications (amplification electrical signals in the electrical-optical-electrical signal transduction process). Organic electro-optic materials afford a number of other advantages including exceptional bandwidth (> 100 GHz), low temperature solution (spin casting) and melt (nano-imprint and soft lithography) processing of thin film devices, adaptability to production of conformal and flexible device structures, and compatibility with a diverse array of materials and material technologies including silicon photonics. This last advantage has permitted integration of organic electro-optic materials with silicon photonic circuitry resulting in low power, high bandwidth electro-optic modulation, optical rectification, and all-optical modulation. The last two phenomena relate to the concentration of optical power in the reduced dimensions of silicon photonic circuitry. Another recently demonstrated advantage of organic electro-optic materials relates to terahertz applications, where the combination of the large electro-optic coefficients and absence of attenuation by phonon modes permits development of highly efficient and broad bandwidth terahertz sources and detectors.

This chapter focuses on introducing the reader to critical concepts in the design of organic electro-optic materials and the integration of these materials into new device platforms that promise a new generation of applications for electro-optic technology. Advances in quantum and statistical mechanical numerical methods have facilitated the design of improved materials. The focus of this chapter will not be on the mathematical details of such calculations but rather to understand the definition of critical structure/function relationships derivative from these calculations. The objective is to demonstrate clear paradigms for further improvement of electro-optic activity.

In the course of the discussion, a new class of organic electroactive materials, binary chromophore organic glasses (BCOGs), will be introduced. These materials exhibit enhanced electro-optic activity, reduced optical loss, and enhanced stability (both thermal and photochemical) in agreement with the predictions of theory. Such BCOGs permit control of both electronic charge perturbation (relevant to nonlinear optical behavior) and transport (relevant to electronic, photovoltaic, light-emitting, and photorefractive behavior) and as such may have broader relevance to electronic, photonic, and optoelectronic behavior. Electrical conductivity in electro-optic materials is critical to several aspects of electro-optic device performance including bias voltage stability.

This chapter provides a tutorial on intermolecular electrostatic interactions in non-ionic materials, which should be of interest and utility to advanced undergraduate, graduate, and postgraduate students in chemistry, physics, and materials science for understanding a variety of photonic, optoelectronic, and electronic phenomena. The device concepts and material specifications should be of interest to electrical and optical engineers, particularly those focused on "Beyond Moore's Law" information technology and a variety of technologies ranging from phased array radar to embedded network sensing.

1.1 Acknowledgments

The authors gratefully acknowledge financial support provided by the National Science Foundation (DMR-0551020 and DMR-0120967) and by the Air Force Office of Scientific Research. Helpful discussions and technical assistance provided by members of the Prezhdo, Scherer, and Jen research groups are also gratefully acknowledged as are many helpful discussions with Oleg Prezhdo (University of Washington), Michael Hayden (University of Maryland, Baltimore County), Axel Scherer (California Institute of Technology) and Alex Jen (University of Washington).

Chapter XX
Organic Photonic Materials

Larry R. Dalton, Philip Sullivan, Denise Bale, Scott Hammond, Ben Olbricht, Harry Rommel, Bruce Eichinger, and Bruce H. Robinson

University of Washington, Department of Chemistry, Seattle, WA 98195

1.3 Introduction

An often stated advantage of organic materials for nonlinear optics is the virtually limitless ability to improve performance by synthetic modification of both chromophores (individual molecules) and material structures (supermolecular organization of molecules). However, for synthetic improvement of nonlinear optical materials to be accomplished in a timely manner, material design must be driven by a quantitative knowledge of critical structure/function relationships. Quantum and statistical mechanical calculations are required for a "first principles" definition of structure/function relationships

at both the molecular and macroscopic levels. Quantum mechanical calculations are most commonly carried out considering isolated molecules; and properties, such as molecular first hyperpolarizability, are calculated in the long wavelength limit. In contrast, experimental measurement of molecular optical nonlinearity (e.g., molecular first hyperpolarizability) is typically carried out on molecules in dielectric media and at finite measurement (optical) frequencies. Moreover, macroscopic properties have commonly been estimated considering chromophores acting as independent particles (no intermolecular electrostatic interactions). In practice, molecules with substantial hyperpolarizability usually experience strong intermolecular electrostatic interactions that strongly influence the macroscopic order and dielectric permittivity of materials. Thus, meaningful direct correlation of experiment and theory has not been possible in the past, inhibiting the systematic improvement of materials. Here we are interested in understanding the role of such strong intermolecular electrostatic interactions in defining the properties of complex photonic materials and using that knowledge to prepare new materials with dramatically improved properties. Stated in other terms, we are interested in a first principles understanding of optical nonlinearity from molecules to materials.

We are also interested in understanding the role of device structure in defining performance in nonlinear nonlinear optical applications.. In particular, we are interested in resonant device structures, silicon photonics, and sub-λ photonic phenomena. We will demonstrate that organic nonlinear optical materials can be combined with silicon photonic structures, with nanoscale critical dimensions, to achieve dramatically improved performance related to electro-optic modulation, optical rectification, and all-optical modulation.

To make our discussion as concrete and concise as possible, we largely limit our discussion to second order nonlinear optical materials and particularly to dipolar chromophores and electro-optic materials prepared by the electrical poling of dipole chromophores in various material lattices at temperatures near the glass transition temperatures of the materials. Such second order materials are particularly attractive in that they have only two non-zero components for the second order nonlinear optical tensors (e.g., r_{33} and r_{13} for the electro-optic tensor relevant to the interaction of optical and radiofrequency fields in a material). For second order optical nonlinearity to be non-zero for such materials, noncentrosymmetric (acentric) symmetry must apply at both the molecular and macroscopic levels. Indeed, the principal element of the electro-optic tensor, r_{33}, can be related to an acentric order parameter, $\langle\cos^3\theta\rangle$ by

$$r_{33} = \beta(\omega,\varepsilon)N\langle\cos^3\theta\rangle\text{constant}(n,\varepsilon) \qquad (1)$$

where $\beta(\omega,\varepsilon)$ is the molecular first hyperpolarizability (which depends upon optical frequency, ω, and material dielectric permittivity, ε), N is the chromophore number density (molecules/cc), and n is the index of refraction. The three angles of the acentric order parameter relate the principle axes of the high frequency optical field, the low frequency radiofrequency field, and the

material electro-optic tensor. In the above equation, chromophore number density and acentric order parameter are not independent; rather, the dependence of $\langle\cos^3\theta\rangle$ on N is defined by intermolecular electrostatic interactions. Thus, the problem of maximizing r_{33} can be thought of as a two-fold process of optimizing $\beta(\omega,\varepsilon)$ and optimizing $N\langle\cos^3\theta\rangle$. Of course, ε depends upon N so the variables of Eq. (1) are quite inter-dependent. Indeed, $\langle\cos^3\theta\rangle$ can also be influenced by material conductivity which, in turn, can depend in a complex manner on N. Conductivity acts to influence the effective poling field felt by the chromophores. Device performance, e.g., bias voltage drift, can also be influenced by material conductivity. From these comments, the importance of a unified and quantitative understanding of the factors that influence electro-optic activity is evident.

Quantum mechanical calculations, including density functional theory (DFT) and time-dependent density functional theory (TD-DFT), have proven useful in predicting trends in linear and nonlinear optical properties.[1-10] In the following sections, we focus on understanding dielectric and frequency effects necessary to arrive at an understanding of the absolute values electro-optic coefficients and not just trends.

State-of-the-art organic electro-optic materials are most commonly composed of chromophores with ground state dipole moments between 10-15 Debye. Clearly, strong intermolecular electrostatic interactions will exist among these high dipole moment chromophores at moderate (>2-3 x 10^{20} molecules/cc) chromophore number densities. A number of approximate treatments have been developed for considering intermolecular electrostatic interactions that are comparable to chromophore-poling field interactions and to thermal energies. One approach has been to develop analytical expressions for the potential function describing the effective electrostatic field felt by a reference chromophore from a surrounding ensemble of strongly interacting chromophores.[11-13] This leads to a multiplicative attention factor for the acentric order parameter given by $[1 - L(W/kT)^2]$, where L is the Langevin function, W is the intermolecular electrostatic interaction energy, and kT is the thermal energy. In this approach, we have followed the work of Piekara[14] but we have used analytical potential functions with approximations ranging from the point dipole approximation, to a hard object treatment of nuclear repulsive effects, to classic 6-12 potential function treatments. Even our most approximate (point dipole) treatments correctly predict the qualitative variation of electro-optic activity with chromophore number density, namely, that electro-optic activity is predicted and observed to go through a maximum with increasing number density. The maximum in the plot of r_{33} versus N is predicted and observed to vary as $N_{max} \propto kT/\mu^2$. Incorporation of the effect of nuclear repulsive interactions into calculations is required to quantitatively predict the behavior of acentric order parameter with number density. More recently, the effect of intermolecular electrostatic interaction on the order of electrically-poled organic materials has been addressed by atomistic Monte Carlo/molecular dynamic[15-17] and pseudo-atomistic Monte Carlo[18-21] calculations. There is reasonable agreement between various approaches with respect to reproducing trends in the variation of electro-

optic activity with structure and with chromophore number density. The recent research of Robinson and Rommel[20,21] is particularly enlightening in predicting that spherically-shaped chromophores represent an optimum shape for maximizing the electro-optic activity of chromophore/polymer composite materials. They have considered both "on-lattice" (where a uniform spatial distribution of chromophores is an imposed condition of the calculation) and "off-lattice" (where chromophores are permitted to assume a non-uniform spatial distribution) calculations of the variation of electro-optic activity with number density for different chromophore shapes. Both on-lattice and off-lattice calculations predict that maximum achievable electro-optic activity will increase as the major to minor axis ratio of prolate ellipsoid chromophores is decreased to unity (the case of a sphere). The predictions deriving from on-lattice and off-lattice calculations differ when progressing from spheres to oblate ellipsoids. On-lattice calculations predict oblate ellipsoid shaped chromophores to exhibit larger maximum achievable electro-optic activity than possible with spheres while the converse is true for off-lattice calculations. Unfortunately, synthetic chemists have not, to the present, produced chromophores with wide variation in general shape and particularly have not produced chromophores with oblate ellipsoidal shapes that represent good approximations to the theoretically considered shapes. Thus, a good test of the predictability of on-lattice and off-lattice calculations for oblate chromophores does not exist at this time. The trends observed in going from prolate shapes to spheres appear reasonably well reproduced.

While studies aimed at understanding chromophore/polymer composite materials have provided good insight into optimizing electro-optic activity for these materials, quantitative prediction of electro-optic activity has been elusive due to the influence of medium dielectric permittivity on electro-optic activity and the variation of electro-optic activity with optical frequency (dispersion effects). In this chapter, we will demonstrate how such effects can be rigorously considered. Moreover, we will extend theoretical consideration to materials more complex than simple chromophore/polymer composites. In particular, we will consider multi-chromophore-containing dendrimer materials (where the presence of covalent bonds influence poling-induced order), binary chromophore organic glasses (BCOGs), and complex organic electro-optic materials prepared by optically-assisted poling. Although we have not (at this time) rigorously investigated the latter two classes of materials, we can report preliminary experimental measurements (and some course-grained theoretical calculations) that are highly suggestive concerning routes to optimizing electro-optic activity. Indeed, these preliminary studies have led to electro-optic coefficients (measured at telecommunication wavelengths) as high as 450 pm/V and these measurements suggest route to further substantial improvement of electro-optic activity and auxiliary properties such as optical loss. The chronological improvement of molecular and macroscopic second order optical nonlinearity is shown in Fig. 1. In this figure, data are limited to materials that have been used to fabricate prototype devices. Marks and coworkers[7] have recently reported "twisted"

chromophores exhibiting even larger values of molecular first hyperpolarizability than the chromophores in the materials of Fig. 1. However, the chromophores of Marks and coworkers have not be incorporated into device relevant materials at the time of this writing. From Fig. 1, it is clear that the rate of improvement of electro-optic activity exceeds that expected from a Moore's Law plot. Recently, the Defense Advanced Projects Research Agency (DARPA) has launched the supermolecular photonics (MORPH) program. The phase II goal of this program is an electro-optic activity of 600 pm/V (indicated by the star in Fig. 1). The structures of representative electro-optic chromophores are shown in Fig. 2 and the structure of several chromophore-containing dendrimers and polymers are shown in Fig. 3. Binary chromophore organic glasses are formulated by combining a chromophore guest with a chromophore-containing host; several examples are shown in Fig. 3 and will be discussed in this chapter.

1.4 Effects of Dielectric Permittivity and Dispersion

In this section, we demonstrate that DFT methods lead to a quantitative understanding of the dependence of β on ε and ω. As noted above, an obstacle to the quantitative correlation of theory and experiment for molecular first hyperpolarizability, β, and electro-optic activity, r_{33}, is the dependence of the properties on dielectric permittivity, ε, and optical operating frequency, ω. We have recently carried out experimental and theoretical investigations of these dependences. Femtosecond time-resolution, wavelength-agile Hyper Rayleigh Scattering (HRS) measurements[22] on chromophores in different media were used to investigate the dependence of β on ε and ω. These measurements were complemented by electric field induced second harmonic (EFISH) measurements[23,24] of the product of chromophore dipole moment, μ, and molecular first hyperpolarizability, β. Modified Teng-Man ellipsometry[25,26] and attenuated total reflection (ATR)[26,27] were used to measure electro-optic coefficients (tensor elements) (see Fig. 4). Measurements of electro-optic coefficients were also carried out in device geometries including Mach Zehnder interferometers and ring microresonators.[28-31] Calculations of β were carried out employing DFT or TD-DFT methods. Calculations of acentric order were effected employing pseudo-atomistic Monte Carlo methods. The chromophores and macromolecular materials that are the focus of this chapter are summarized in Figs. 2 and 3. The ability of density functional theory methods to simulate the variation of $\mu\beta$ with ε is illustrated in Table 1. We have used two DFT approaches (Gaussian B3LYP/3-21g*PCM and Dmol using PBE/dnp/Cosmo) to investigate the dependence of β on ε. $\beta_{zzz}(\varepsilon)$ is predicted vary linearly with $(\varepsilon - 1)/(\varepsilon + 2.5)$ in contrast to the predicted Onsager dependence, $\beta_{zzz}(\varepsilon) \propto (\varepsilon - 1)/(\varepsilon + 2)$. The two DFT methods predict a linear dependence for the variation of dipole moment, μ, with $(\varepsilon - 1)/(\varepsilon + 1)$. A discussion of dielectric permittivity measurements is given in the thesis of Scott Hammond.[32] DFT calculations also

predict that the dependence of molecular first hyperpolarizability upon measurement frequency, ω, will be different than that predicted by the two-state model (see Fig. 5), namely, that the simple two-level approximation tends to over-estimate β values at optical measurement frequencies. Table 1 illustrates how the understanding of the dependence of β on ε and ω translates to improved correlation of theory and experimental data.

1.5 Complex Dendrimer Materials: Effects of Covalent Bonds

Covalent bond potentials have a strong effect on the rotation and spatial organization of chromophores in complex structures such as dendrimers (see Fig. 3). Fully-atomistic MC/MD methods[15,16] provide an attractive path to consideration the effects of covalent bonds; however, when applied to systems of the complexity of those of Fig. 3, such calculations become difficult to execute in a time and cost effective manner. This dilemma can be circumvented by adapting the course-grained models of our previous work to a "pseudo-atomistic" MC approach.[18-21] Since π-conjugation inhibits internal rotation, π-electron segments can be effectively treated within the United Atom Approximation (see Fig. 6). Quantum mechanics are employed to define the charge distributions over these "United Atom Ellipsoids" in a manner analogous to fully-atomistic methods. Sigma-bonded regions of dendritic and polymeric structures are treated in a fully atomistic manner (Fig. 6); thus, we refer to this computational methodology as a "pseudo-atomistic" approach. The details of the computations are presented elsewhere.[20,21,33] The focus in this chapter is on the important conclusions derivative from such calculations. An obvious requirement of theory is that it must correctly predict electric field poling behavior and this is, indeed, seen to be the case in Fig. 7, where a linear dependence on poling voltage is predicted. A linear dependence is experimentally observed for the PSLD-33 dendrimer material (Note that the structure of the PSLD-33 dendrimer is the same as the PSLD-41 without the outer Frechet dendrons). Because electro-optic activity (r_{33}) increases linearly with electric poling field strength (E_p), it is useful to report the variation of r_{33}/E_p with number density, N, where each r_{33}/E_p has been obtained by linear least squares fitting of the variation of r_{33} with E_p.

The results of applying pseudo-atomistic Monte Carlo methods to the two dendrimers (PSLD-33 and PSLD-41) of Figs. 3 and 6 are shown in Fig. 8**.** Chromophores within these dendrimer materials act as independent particles, i.e., electro-optic activity increases linearly with chromophore number density implying that the acentric order parameter is independent of chromophore concentration. Intra-dendrimer chromophore organization is strongly influenced by covalent bond potentials and acentric order at low concentrations is less than that observed for the same chromophore (an FTC-type chromophore—see Fig. 2) in a polymer such as amorphous polycarbonate (APC). We have used polarized absorption spectroscopy[34] to independently measure order for the materials of Fig. 8. The results are consistent with the theoretical predictions shown in Fig. 8, i.e., with a $\langle\cos^3\theta\rangle \sim 0.08\text{-}0.12$ depending on poling voltage. Note also that

$r_{33}/E_p = 1.33$ and $\langle P_2 \rangle / E_p = 1.33$ for PSLD-33 indicating the typical agreement between electro-optic and polarized absorption spectroscopy for determining the field dependence of chromophore order. The measured ratio $r_{33}/r_{13} \approx 3$ (from ATR measurements) is also consistent with low acentric order.

Multi-chromophore-containing dendrimers do permit high chromophore loading to be achieved without phase separation or centrosymmetric crystallization. Indeed, the maximum electro-optic activity that can be achieved with these materials exceeds that which can be obtained for the same chromophore in chromophore-polymer composite materials (because the roll-off with increasing N is avoided). However, results to the present do not suggest that multi-chromophore-containing dendrimer materials can yield electro-optic coefficients exceeding the Langevin limit.

Multi-chromophore-containing dendrimers permit the dielectric environment of chromophores to be systematically tuned, which can be used to influence both electro-optic and optical absorption (and index of refraction) properties. When functionalized with cross-linking moieties, dendrimers can lead to more homogeneous cross-linking (and thus reduced light scattering) than polymer materials (where a distribution of void volumes is an inherent problem).

The experimental results and conclusions for these multi-chromophore-containing dendrimers are not general for other dendrimer systems. For example, if length of the flexible spacer between the dendrimer core and the chromophores is increased, then the electro-optic behavior approaches that observed for chromophore/polymer composites. These results emphasize that electro-optic activity in complex nano-structured materials such as dendrimers can be quantitatively predicted from first principles calculations.

For the sake of brevity, we have not discussed the details of the synthesis and characterization of the dendrimers discussed above. The reader is referred elsewhere for this detail.[26,35,36]

The important conclusion of this section is that the large electro-optic activities observed for multi-chromophore-containing dendrimers do not arise from high acentric order but rather high chromophore number density and enhancement of molecular first hyperpolarizability by the dielectric permittivity of the environment of dendrimer materials. Indeed, the order parameter is quite small suggesting that further substantial enhancement of electro-optic activity can be achieved by increasing acentric order.

In the preceding, we have demonstrated that strong electronic dipolar interactions, strong nuclear repulsive (steric) interactions, and covalent bond potentials (all of which are spatially anisotropic interactions) can be used to influence the assembly and organization of charge transfer chromophores. We have further demonstrated that the resulting order can be quantitatively understood from first principles quantum and statistical mechanical computations.

1.6 BOCGs: Optimizing EO Activity and Optical Transparency

Binary chromophore organic glasses (BCOGs) are a new class of organic electro-optic materials that affords important control of dielectric permittivity and chromophore acentric order. BCOGs permit very high total chromophore concentrations (number densities) to be realized without the consequences of unwanted phase separation problems or dielectric permittivity changing with chromophore concentration. The absence of chromophore-concentration-dependent solvatochromic (bathochromic or "red") shifts for BCOGs minimizes absorption loss at telecommunication wavelengths. The absence of phase-separation and index of refraction heterogeneity minimizes optical loss due to light scattering. Indeed, BCOGs may ultimately afford a route to "organic crystal engineering" based on solution processed (e.g., spin coated) materials.

A BCOG consists of a "guest" chromophore doped into a chromophore-containing "host" material. One might well expect such doping to lead to greater guest-host compatibility than for doping chromophores into traditional polymer materials such as amorphous polycarbonate (APC) or poly(methylmethacrylate) (PMMA). This is indeed the case. The free energy of mixing of guest and host components of BCOGs should be more favorable from both enthalpic and entropic considerations. With BCOGs, a polar chromophore guest is dissolved in a polar host in contrast to the traditional composite material, which involves dissolving a polar chromophore guest into a non-polar host. The shapes of both guest and host chromophores can be engineered to control steric interactions and thus control chromophore packing and order.

As shown in Fig. 9 for the case of doping the YLD-124 chromophore into PSLD-41, electro-optic activity is observed to increase rapidly (and linearly) with added guest chromophore concentration. The rate of increase is a factor of 2-3 greater than observed for doping the same guest chromophore into a traditional polymer such as APC. Logically, this increase in electro-optic activity arises from an increase in $\beta(\varepsilon,\omega)$ or $\langle\cos^3\theta\rangle$ or a combination of these two effects. To discriminate among these possibilities, we have carried out detailed studies of changes of dielectric permittivity, solvatochromism, and spectral line broadening with guest chromophore doping (number density). The latter two studies involved the use of sophisticated spectral deconvolution techniques for the guest and host chromophores when doping YLD-124 into PSLD-41. Because the conclusions of these studies are dramatically reinforced by the studies reported in the next section involving more first order analysis, we will not discuss spectral deconvolution results here other than to note that essentially no significant solvatochromic shifts or spectral line broadening were observed with increasing guest (YLD-124) chromophore concentration. This is in marked contrast to doping of chromophores into APC as discussed at length by researchers at Lockheed Martin.[37,38] Moreover, we observed the changes in bulk dielectric permittivity to be too small to account for the observed changes in electro-optic activity although a detailed investigation of such effects is continuing. The details of such measurements and analysis will be discussed elsewhere but the

results are consistent with the lack of solvatochromic shifts discussed in the next section.

The electro-optic behavior observed in Fig. 9 (and for many other BCOG systems[39-41]) is striking and implies that the acentric order parameter $\langle\cos^3\theta\rangle$ is either independent of concentration or increases linearly with concentration. Moreover, the rate of increase of electro-optic activity is greater than that predicted from the independent particle approximation and thus intermolecular electrostatic interactions must be acting to enhance poling-induced order if the increases in electro-optic activity are to be assigned to increasing acentric order. We are currently investigating a variety of BCOGs employing the same pseudo-atomistic Monte Carlo approaches discussed in the preceding section. The completion of such studies is critical to a truly meaningful discussion of the various contributing factors to the dramatically improved electro-optic activity observed for BCOGs. However, we have already utilized very course-grained MC calculations, based on the earlier mean field work of Prezhdo and coworkers,[42] to analyze the results presented in Fig. 9. Initial theoretical results are also presented in Fig. 9 and show surprising agreement with the experimental data. These results have been mapped back to fully atomistic MC calculations. The essential conclusions are summarized in the following paragraph.

Theory suggests that specific spatially anisotropic intermolecular electrostatic interactions among guest and host chromophores result in a significant increase in $\langle\cos^3\theta\rangle$. We have examined snap shot pictures of equilibrium chromophore spatial distributions calculated by Monte Carlo methods. One very favorable interaction between guest and host chromophores involves the chromophore-containing host dendrimer (PSLD-41) forming an umbrella or pyramidal shape and the guest chromophore (YLD-124) approaching from the base of the pyramid along the normal to the base. The donor region of the guest chromophore thus experiences a favorable interaction with the acceptor regions of the host chromophores. The strength of this interaction is many times that of the thermal energy, kT. We must immediately note that this is just one of an enormous number of observed interactions and the moderate order observed and calculated cautions against putting too much emphasis on such particularly favorable interactions. Indeed, it might be argued that this is simply a result that is defined by nuclear repulsive interactions or lattice symmetry effects (see Fig. 10). As shown in Fig. 10, reducing the symmetry of the lattice which the chromophore sees from 3-D to 2-D to 1-D is predicted to result in an increase in $\langle\cos^3\theta\rangle$.

The one example where a specific spatial anisotropic interaction may clearly play a significant role is the case of quadrupolar aromatic-H•••aromatic-F quadrupolar dendron interactions reported by Jen and coworkers.[39,40] In these dendrimer materials, long-range "chiral-like" interactions (orthogonal quadrupolar and dipolar interactions) may enhance noncentrosymmetric order. Such interactions also appear to influence material glass transition temperatures and the stability of poling-induced acentric order. This was the first BCOG to exhibit electro-optic coefficients in excess of 300 pm/V, while also exhibiting

optical loss of less than 2 dB/cm and glass transition temperatures greater than 200°C (when crosslinked).

To test the effect of host lattice order on guest chromophore orientation under a poling field and vice versa, we developed an experiment where the order of the host chromophore could be increased by laser-assisted poling (LAP).[43]

1.7 BOCGs: Laser-Assisted Poling (LAP)

The disperse red 1 chromophore-containing polymethylmethacrylate polymer host, (DR-1)-co-PMMA, used for Laser-Assisted Poling (LAP) is shown in Fig. 3 and the YLD-124 guest chromophore used in these experiments is shown in both Figs. 2 and 3. The modification of our Teng-Man apparatus for LAP experiments, using a linearly polarized optical field, is shown in Fig. 4. Fig. 11 shows a typical experiment demonstrating the dramatic increase in electro-optic activity with LAP. LAP should have little impact on bulk dielectric permittivity but is well-known to increase the order of DR-1.[43,44] A comparison of the variation of electro-optic activity with poling voltage is shown in Fig. 12 with and without laser-assisted poling. In Fig. 13, we show the variation of electro-optic activity with YLD-124 concentration with and without laser-assisted poling. Although detailed simulations of this behavior have not yet been completed, there is little doubt that the observed phenomena reflect the influence of guest-host interactions and that LAP provides a systematic way of increasing host chromophore order. More detailed studies should shed greater light on the exact nature of these interactions and on the relationship between guest and host order.

Fig. 14 illustrates another reason for studying the YLD-124/(DR-1)-co-PMMA system. The charge transfer absorption bands of DR-1 and YLD-124 do not overlap so the absence of solvatochromic shifts and spectra line broadening can be directly observed without resorting to spectral deconvolution methods. Enhanced electro-optic activity is observed for BCOGs while at the same time reduced optical loss is observed. This can be explained in terms of the better compatibility between guest and host materials which leads to improved free energy of mixing and thus less phase separation at high chromophore loading. The weak dependence of spectral features on guest chromophore concentration results in reduced contributions to optical loss from both absorption and scattering. Spectral line positions and widths are essentially independent of chromophore concentration for BCOGs. Total material optical loss of 2 dB/cm or less is obtained even for materials with high chromophore loading. For example, the intrinsic thin film optical loss of the AJ415 BCOG (see Fig. 3) is approximately 1.4 dB/cm at 1.55 microns wavelength. Hydrogen vibrational overtone absorptions typically result in optical loss on the order of 1 dB/cm so very little excess loss due to other mechanisms is observed for the AJ415 system.

The LAP YLD-124/(DR1)-co-PMMA materials discussed in the preceding paragraphs are not appropriate for serious device applications because the

material glass transition temperatures are too low. We would need to introduce cross-linking to harden the final material lattice to an acceptable level for device applications. The general principles of lattice hardening will be discussed in a subsequent section of this chapter. While the above system does lead to low optical loss (DR-1 does not make a significant contribution to absorption loss), the electro-optic activity does not exceed that of other BCOGs. The primary reason for this is that the DR-1 chromophore does not make a significant contribution to electro-optic activity even when its acentric order is increased by LAP and interaction with YLD-124 chromophores. Moreover, the aspect ratio of the DR-1 chromophore is not sufficiently large to have an optimum effect on increasing overall order and thus electro-optic activity. Production of practical (for device application) LAP-BCOGs will likely require development of improved LAP host materials that contribute significantly to total electro-optic activity and produce further enhancement of total acentric order. Nevertheless, the current materials contribute significantly to understanding of the effect of guest-host intermolecular electrostatic interactions on electro-optic activity.

LAP BCOG materials may be the most promising route to solution-processed electro-optic materials with exceptional electro-optic activity and desirable auxiliary properties that permit the production of devices with exceptional performance and prerequisite stability. Before we leave this section, let us consider in the most general terms the use of LAP to optimize electro-optic activity. Certain types of chromophores dispersed in media that limit rotational diffusion can be oriented by optical poling. Setting aside the mechanism of the action of the laser field on the chromophore, the effect can be understood through consideration of Le Chatelier's principle: When a stress is applied to a system, the system adjusts itself so as to relieve the stress. When a laser field illuminates a sample containing a chromophore that is capable of absorbing the light and converting the energy into heat, the system will adjust itself so as to minimize the heating. Since the probability for absorption of energy is proportional to the scalar product, $\mu_{ge}E$, of the transition moment, μ_{ge}, and the applied electric field, E, the system can minimize heating if the molecules reorient so that their transition dipoles are orthogonal to the applied field.

In order for this to lead to a useful ordering of the EO materials, the following five conditions are relevant: (1) The excited state must relax back to the ground state *via* librational-vibrational motions. In do doing, the inert matrix surrounding the dipole (chromophore) will undergo local heading, thus facilitating rotational (re-orienting) diffusion of the chromophores. While trans-cis isomerization is implicated as the mechanism for conversion of electronic excitation energy into nuclear motions, there may be other types of relaxation mechanisms, e.g., intersystem crossing, that can accomplish the same thing. (2) The angle between the transition dipole and the ground state dipole vectors is a critical parameter. Assuming for the moment that the optical poling is perfect, the orientation of the molecules relative to the optical field could be anywhere. In practice, the orientation of the optical E field should be independently optimized to maximize the desired EO enhancement. The transition dipole is

calculable with quantum methods. (3) The temperature of the matrix should be as cold as possible while allowing the poling to occur. The local heating that results from absorption of a photon with energy of about 2 eV ≈ 46 kcal/mol is sufficient to heat about 500 atoms to a temperature on the order of 45 K. By maintaining the temperature of the sample this much below the glass transition temperature of the matrix, the poling efficiency should be maximized. This order of magnitude estimate seems to be reasonable relative to experiments—for systems investigated to date the optimum temperature appears to be approximately 30 K below the glass transition temperature. Once the chromophore has rotated, the matrix must freeze around it so as to obstruct reversion. Optimally, all of the chromophores will have rotated "into the shade" so as to align their transition dipoles orthogonal to the applied optical field, and they will not relax back when the optical field is removed because the matrix is sufficiently rigid to prevent rotational diffusion. Experimentally, the optimum poling temperature is defined by investigation of the temperature and optical power that leads to maximum electro-optic activity using *in situ* monitoring of the experiment (see Fig. 4). (4) The optical poling must be done in the presence of an external static electric field so as to break the symmetry of the applied laser field. (5) Plane polarized light will orient the transition dipoles in a plane orthogonal to the plane of the electric vector (two dimensional Bessel order). If circularly polarized light is used, the transition dipole will be oriented orthogonal to the plane of the rotation (one-dimensional Ising order of the transition dipoles).

1.7 BOCGs: Conductivity Issues

James Grote and coworkers[45-50] have, for some time, pointed out the critical issue of the relative conductivities (or conversely, resistivities) of electro-optic core and cladding materials for the fabrication of multi-stack (bottom electrode-bottom cladding-EO core-top cladding-top electrode) electro-optic devices. The resistivity of the electro-optic core must be higher than that of the cladding materials if voltage is to be dropped across the core material. If this condition is not met, poling efficiency will be dramatically compromised and drive voltage requirements of devices will be increased.

Under the best of circumstances, this is not an easy requirement to satisfy. The index of the refraction of cladding materials must be less than that of the electro-optic waveguide materials so that light propagating in the electro-optic core material is prevented from interacting with metal electrodes. Such interaction would lead to unacceptable optical loss. The index of refraction condition is easily met due to the presence of π-electron chromophores in the core material. However, these π-electron chromophores can also lead to electrical conductivity under poling conditions and thus it is difficult to simultaneously satisfy relative conductivity and index of refraction requirements of core and cladding materials. Efforts to increase the conductivity of the

cladding materials have also led to cladding materials with increased optical loss. Among the most successful efforts to improve the conductivity of cladding materials without unacceptable side effects is that of Peyghambarian and coworkers working with sol gel glass materials; these researchers has also addressed this issue by exploiting novel device structures.[51-54] Another route to dealing with core-cladding issues is to pursue electric field poling and device operation using coplanar electrodes, which has been pioneered by Steier and coworkers.[55]

An effort has also been made to address this issue by developing improved transparent metal oxide conducting electrode materials.[56,57] However, the conductivity of such electrodes is low compared to gold or copper electrodes and this can result in severe bandwidth limitations for devices as bandwidth is currently defined by the resistivity of drive electrodes. Moreover, the optical loss of transparent metal oxide electrodes has been unacceptably high at telecommunication wavelengths. This, like the development of conducting cladding materials, remains a critical research challenge for realization of high performance electro-optic devices based upon utilization of organic electro-optic core materials.

The problem of conductivity is particularly problematic for BCOG materials and indeed currently limits the performance of these materials, which would be truly spectacular in the absence of this problem. This is illustrated in Figs. 15 and 16 where conductivity is shown to limit poling efficiency by defining the maximum effective electric poling field that can be realized across the electro-optic thin film material. As seen in Fig. 16, the electric field at which "run away" conductivity occurs decreases with increasing chromophore concentration (number density) for BCOG materials. Conductivity in BCOG materials results from variable range charge hopping between chromophores and this can obviously relate to the spatial separation and relative orientation of chromophores. One future way to decease this unwanted effect for materials with high chromophore number densities may be to sterically protect chromophores with "insulating" substituents. Otherwise, one is faced with working at lower chromophore number densities.

To illustrate the severity of conductivity at the present, it can be noted that electro-optic activity would be doubled in BCOGs if poling fields could be increased to normal values of 120 volts/micron. The problem is even more severe for poling of multi-stack device structures. If this problem could be solved, it is clear that high bandwidth electro-optic devices could be fabricated with operating voltages on the order of 100 millivolts with no further improvements in chromophore molecular first hyperpolarizability.

1.8 Thermal and Photochemical Stability: Lattice Hardening

Materials having glass transition temperatures between 100 and 200°C afford many advantages for processing. Not only are such temperatures attractive for

avoiding chromophore decomposition during electric field poling but such temperatures permit use of soft and nano-imprint lithography techniques for the fast and low cost fabrication of complex optical circuitry. However, such relatively "soft" materials are not suitable for producing devices that surpass Telcordia standards (e.g., long term operational stability at 85°C).

To satisfy Telcordia standards for thermal stability, a high glass transition temperature material is required. Typically, this condition has been satisfied by employing a high glass transition temperature host, such as a polyimide or polyquinoline polymer, to fabricate composite materials or by effecting cross-linking of materials subsequent to induction of acentric order by electric field poling. Cross-linking chemistries are also frequently used to harden cladding materials, e.g., UV-curable epoxies are commonly used as cladding materials.

Use of a high glass transition temperature polymer as a host for the preparation of electro-optic composites has a number of drawbacks. The high processing temperatures (200°C and greater) required for such materials can lead to sublimation of chromophores and to chromophore decomposition. Moreover, harsh solvents are often required for spin casting of such materials leading to poor optical quality films and high optical loss.

Lattice hardening subsequent to poling has become an attractive option permitting low temperature processing through spin casting and poling stages and then permitting a high glass transition temperature material to be generated at the end of the poling process. Prior to 2000, most cross-linking protocols focused on condensation reactions (e.g., urethane chemistry) or radical addition reactions.[58,59] Photo-induced cross-linking chemistries were pursued without much success because of competition of organic electro-optic chromophores and cross-linking initiators for light.

A breakthrough in lattice hardening occurred with the introduction of two cycloaddition reactions: (1) The Diels-Alder/Retro-Diels-Alder reaction[36,40,60,61] involving dienes and dienophiles and (2) the thermally-initiated soft free radical reaction of the fluorovinyl moiety to yield cyclobutyl cross-links.[62-65] The latter reaction was popularized by Dennis Smith and his colleagues at Dow Chemical and Clemson.[65] Both cycloaddition chemistries are thermally activated. Both approaches have yielded hardened electro-optic materials exhibiting glass transition temperatures on the order of 200°C. The resulting hardened materials meet and surpass Telcordia standards for thermal stability. Such lattice hardening also improves photostability.

An advantage of the Diels-Alder/Retro-Diels-Alder reaction is that processing temperatures and the reversibility of the cycloaddition reaction can be controlled by the choice of diene and dienophile reactants and a number of choices are possible (see Fig. 17). The UV curing of cladding materials in triple stack (lower cladding-EO core-upper cladding) devices can be problematic for electro-optic materials containing cycloaddition precursors. For example, reaction of the radicals from the cladding materials with the anthracene diene can produce anthracenyl radicals that can attack chromophores and disrupt the stoichiometry of the Diels-Alder reaction.

Another problem associated with the use of crosslinkable electro-optic materials arises when poling is carried out through cladding layers. Because the core electro-optic material is not hardened when the upper cladding layer is deposited, the deposition process associated with the upper cladding layer can influence the surface smoothness of the electro-optic core waveguide leading to light scattering and unacceptable optical loss. Moreover, if the glass transition temperatures of the cladding layer is not much higher than the core, the two may inter-diffuse during poling. Several options exist for circumventing this problem including corona poling and lattice hardening followed by cladding layer deposition. Alternatively, electrode (parallel plate or coplanar) poling can be carried and the electro-optic material hardened followed by removal of the electrodes, deposition of the upper cladding layer and the upper electrodes.

When speaking of thermal stability, a distinction should be made been the stability of poling-induced order (which relates to the final glass transition temperature of the material) and the thermochemical stability of molecular components of the electro-optic material. Normally for use in the production of electro-optic materials, chromophores are required to exhibit thermochemical stability greater than 250°C. Thus, the thermal stability of devices usually relates to the glass transition temperature of the electro-optic material, which is on the order of 200°C or somewhat lower..

Photochemical stability is equally as important as thermal stability and organic electro-optic materials must be capable of withstanding power levels used in telecommunications (currently, 10-20 mW) for many years.

1.9 Thermal and Photochemical Stability: Measurement

The modified Teng-Man apparatus of Fig. 4 is very effective for measuring thermal stability since the temporal stability of electro-optic activity can be continuously measured at various elevated temperatures. Thermal stability is also conveniently measured by ramping temperature and observing the temperature at which electro-optic activity is first observed to decrease (see Fig. 18 for an example).[66] Such measurements permit the activation energies for rotational relaxation to be quantitatively defined as discussed elsewhere.[66] Insight into thermal stability can also be obtained by measurements of material glass transition temperature by thermal analysis (differential scanning calorimetry (DSC)) methods and by measurement of the temperature-dependence of conductivity (see Fig. 16), which reflects the temperature at which the lattice first begins to soften. The glass transition temperature measured by DSC is frequently observed to be higher than that measured by Teng-Man or conductivity measurements. This is because the former reflects overall melting while the latter can reflect local melting (molecular motion such as torsional motion). Such glass transitions and pre-transitions are common in complex organic materials such as polymers and lipid bilayer materials. The pre-transition is more relevant to definition of the thermal stability of electro-optic activity as this pre-transition can lead to significant loss of electro-optic activity. With

cross-linked materials it is not uncommon to observe a stepped loss of electro-optic activity in thermal ramping experiments; this observation typically reflects heterogeneity in cross-link density.

Stability studies can also be carried out on devices and recently Ashley, Lindsay, and coworkers[67] have conducted an interesting study of the FTC and CLD chromophores (see Fig. 2) incorporated into APC and polyimide polymer hosts. In their studies, the change of drive voltage (V_π) is recorded as a function of time. Their conclusion is that multi-year operational stability is possible with the materials that they studied.

Photochemical stability can also be assessed in device structures but a more useful method appropriate for mechanistic studies is shown in Fig. 19. Some representative results are presented in Table 2. This pump-probe method permits accelerated photo-degradation studies to be conducted using pump powers up to 1 watt. Even at the highest pump power levels, rates of photochemical decay are slow so that single experiments must be conducted over periods of days. Because of long measurement times, care must be exercised to insure that the optical probe power does not influence measurements.

It is generally recognized that the dominant mechanism of photochemical decay in organic electro-optic materials (and other organic electroactive materials) involves singlet oxygen chemistry.[68-75] No direct bond breaking or two-photon activated processes are observed with currently employed power levels (or even in high pulse power, femtosecond pulse experiments). Stegeman and coworkers[69-72] have demonstrated most of the critical features of photo-decomposition of organic electro-optic materials including the absence of contributions from multi-photon absorption. They have defined a single photostability figure-of-merit, B/σ, where B^{-1} is the probability of photo-decay from the LUMO (lowest unoccupied molecular orbital) charge transfer state and σ is the interband (charge transfer) absorption coefficient. This definition has been used by subsequent researchers although the data analysis of Stegeman and coworkers may have been somewhat overly simplistic with the consequence of over estimating photo-instability. For example, more detailed analyses demonstrate that the decay data cannot be fit with a single exponential[75] (note that two singlet oxygen species, $^1\Delta$ and $^1\Sigma$, may influence decay kinetics as well as slower non-singlet oxygen mechanisms) and that "observer" power in the Stegeman pump-probe experiments may lead to artificially fast decay. Moreover, Stegeman and coworkers failed to carry out measurements at telecommunication wavelengths; this was addressed in subsequent work by researchers at Corning[73,74] and elsewhere.[75] The Corning group demonstrated that the photostability FOM for a given chromophore structure could vary over four orders of magnitude depending on conditions that influence singlet oxygen chemistry. Even larger variation has been observed by other groups and photostability has been shown to improve with use of small quantities of singlet oxygen quenchers (see Table 2). In addition to pump-probe experiments carried out by Stegeman and coworkers, researchers at Corning, Gunter and coworkers, and Dalton and coworkers, photostability has also been investigated in operating

Mach Zehnder devices by Steier and coworkers and by Ashley and coworkers. Again, in these studies, photo-instability could be attributed to singlet oxygen chemistry with improved photostability being observed for materials and devices where this chemistry was partially inhibited (by partial exclusion of oxygen, i.e., by rudimentary packaging).

In summary, it appears that reasonable photostability can be achieved with appropriate materials modification or with appropriate packaging of devices to minimize the presence of oxygen. In this latter regard, the problems faced with organic electro-optic materials are analogous to those faced with organic light emitting device (OLED) materials. It should be noted that dense crystals such as DAST (4-dimethylamino-N-methyl-4-stibazolium tosylate) exhibit excellent photostability again consistent with the role played by singlet oxygen chemistry in photodecomposition.

When space applications of electro-optic materials are being considered, radiation hardness may be important (depending on how electro-optic devices are packaged and where they are located in satellites). Few studies of the stability of organic electro-optic materials in the presence of high energy radiation have been published but the one published study suggests reasonable stability in the presence of high energy gamma rays and protons.[76]

2.0 Devices and Applications

A distinct advantage of organic electro-optic materials relative to their crystalline inorganic counterpart is their processability and ability to be integrated with a diverse range of materials. Conformal and flexible devices have been fabricated by lift-off techniques and these devices exhibit excellent retention of performance properties (drive voltage, bias voltage, insertion loss) with repeated and extreme flexing and bending.[77]

In addition to standard reaction ion etching (RIE)[78] and photolithographic techniques,[58] devices (e.g., Mach Zehnder modulators and ring microresonators) can be fabricated employing nano-imprint and soft lithography techniques.[79,80] Organic electro-optic materials have also been incorporated into silicon photonic devices including ring microresonators[31] and Mach Zehnder device structures.[81]

Three fundamental device structures have been commonly investigated. These include (1) stripline waveguide structures such as Mach Zehnder and birefringent modulators; (2) resonant structures such as ring microresonators, etalons, and (3) prisms including superprism structures. With stripline devices, a critical device performance parameter is the voltage required to effect modulation or switching. For a Mach Zehnder modulator, the parameter is the drive or V_π voltage (the voltage required to produce a π phase shift in light passing through the device). This is the voltage required to effect optimum transduction of electrical signal information onto an optical carrier as an amplitude modulation. The operational equation is $V_\pi = \lambda h/n^3 r_{33} L\Gamma$ where λ is the operating wavelength, h is the electrode spacing, L is the electrode length, and Γ is the modal overlap parameter. If a push-pull Mach Zehnder interferometer structure is employed a

factor of 2 should be added to the denominator of the V_π equation. Because of the dependence of bandwidth on the resistivity of metal electrodes, choice of electrode length will impact both bandwidth and drive voltage. Device length will also influence insertion loss. A more detailed discussion of performance trade-offs with device designs is given elsewhere[82] but if one assumes for typical material and device dimension values r_{33} = 300 pm/V, h = 8 microns, microwave electrode (gold) loss = 0.75 dB(GHz)$^{1/2}$/cm, fiber coupling loss = 0.8 dB/facet, material waveguide loss = 2 dB/cm, L = 5 mm, then V_π = 0.75 V, 3 dBe bandwidth = 90 GHz, and total insertion loss = 2.6 dB. Clearly, the large electro-optic activity coefficients of organic materials permit superior performance to be realized in each of the critical areas of device performance (drive voltage, bandwidth, insertion loss). Significantly reduced device dimensions also afford advantage, particularly when integrating electro-optic device technology with electronic and photonic circuitry. Drive voltage expressions for other stripline device configurations are discussed elsewhere.[83]

An analogous equation exists for prism and cascaded prism device structures. For such devices, the critical performance parameter is $\theta = (n)^3 r_{33} (VL/dh)$ where L and h are the length and width of the prism or the array of prisms,[84,85] V is the voltage applied across an overall thickness d (or the electrode spacing). In a cascaded prism device, L is the length of the base of the prism cascade. Again, it can be seen that smaller devices can be used if electro-optic activity is sufficiently high.

For resonant devices, such as ring microresonators[86,87] and etalons[53], drive voltage and bandwidth performance cannot be separated. The quality, Q, factor (number of times light transits the resonant structure before being lost) influences both; drive voltage and bandwidth decrease with increasing quality factor. A critical performance factor for resonant devices is the bandwidth/voltage sensitivity factor. The best value for this factor currently obtained with organic electro-optic materials (incorporated into silicon photonic ring microresonators) is approximately 18 GHz/V, which means that the bandpass notch (see Fig. 20) associated with the ring microresonator is tuned by 18 GHz with application of a voltage of 1 volt. To effect optical amplitude modulation employing resonant device structures, the bandpass (notch filter) must be shifted on the order of a full width at half maximum. Enhanced performance is observed for organic electro-optic/silicon photonic ring microresonators relative to all-organic devices due to optical field concentration and reduced electrode spacings.[87] Indeed, optical field intensities are sufficiently great in organic electro-optic material filled 70 nm slots of slotted silicon waveguides that optical rectification is observed with milliwatt and even microwatt input powers.[87] Millivolt electro-optic modulation[88] is possible with such devices and these devices can be used as the fundamental active elements of reconfigurable optical add/drop multiplexers/demultiplexor (ROADM) chipscale routing systems.[89]

Another example of an application exploiting optical rectification is terahertz electromagnetic generation and detection.[90,91] While lithium niobate (device-relevant electro-optic coefficient of 30 pm/V) is the benchmark for

electro-optic modulation applications, zinc telluride (device-relevant electro-optic coefficient of 4 pm/V) is the benchmark to terahertz technology based on high pulse power, femtosecond pulses. In addition to affording significant advantage associated with greater electro-optic activity, organic materials afford dramatically improved bandwidth (currently, terahertz generation and detection is demonstrated to 12 THz but 30 THz may be possible). The improved bandwidth performance is associated with the absence of loss in specific THz spectral regions associated with the phonon modes of crystalline ZnTe. Organic electro-optic materials also afford more facile phase-matching of optical and THz waves leading to dramatically improved sensitivity. The most serious difficulty currently experienced in using organic electro-optic materials for THz applications is the requirement of fabricating thick (millimeter rather than micron thick) films. If this processing change can be overcome, organic electro-optic materials could facilitate the production of compact THz spectrometers.

Applications of organic electro-optic materials are broad, ranging from optical gyroscopes, to phased array radar, to GHz A/D conversion, to digital signal processors, to acoustic spectrum analyzers to sensors.[92-98] Sensing applications are receiving increasing attention.[99]

2.1 Summary and Conclusions

Organic electro-optic materials currently exhibit a number of advantages relative to their inorganic counterparts (e.g., lithium niobate, zinc telluride, etc.). These include greater electro-optic activity, faster response time, superior processability facilitating the mass production of sophisticated and highly integrated (including 3-dimensional) circuitry, improved compatibility with a diverse range of materials, and potentially lower cost. Crystalline inorganic electro-optic materials retain advantage with respect to optical loss and stability. Note that these two advantages of inorganic electro-optic materials do not hold for inorganic electro-absorptive materials.

A distinct advantage of organic electro-optic materials is that properties can be further dramatically improved by molecular and supermolecular engineering. For example, it is likely that the hyperpolarizability of chromophores will be further improved, perhaps by more than an order of magnitude. In like manner, the acentric of order of organic electro-optic materials can obviously be further improved and perhaps “crystalline” organic electro-optic materials can be produced by theoretically-inspired design. In this communication, we have presented several paradigms for the improvement of electro-optic activity including the special intermolecular electrostatic interactions of binary chromophore organic glasses, laser-assisted electrically-poled BOCGs, and self-assembly/sequential synthesis of materials in nanoslot silicon waveguides. It is within the realm of possibility that electro-optic coefficients of “purely electronic” organic EO materials can be increased to values competitive with liquid crystalline materials, while retaining the very fast response times and advantages of robust thin solid (hardened) films. Auxiliary properties of organic

electro-optic materials are also likely to be further improved. Optical loss values as low as 0.1-0.2 dB/cm have been observed for "proton-deficient" dendrimer materials exhibiting optical nonlinearity comparable to lithium niobate. The ability to fine-tune diverse properties of organic electro-optic materials should permit the tailoring of materials to specific device application requirements. Obviously, there are upper limits to the improvement of organic electro-optic materials. Even if crystalline materials can be produced by design, thermal stability will likely be limited to temperatures below 300°C.

In addition to commenting on the potential for future dramatic improvements in material performance, it is useful to speculate on the performance likely achievable within the next couple of years. Electro-optic coefficients in the range 500-1000 pm/V (at telecommunication wavelengths) are highly probable for materials exhibiting optical loss of less than 2 dB/cm and exhibiting stability that satisfies Tedcordia standards. Such materials should permit the fabrication of devices with operating voltages on the order of 0.1 volts (and with bandwidths of > 20 GHz). Indeed, Lumera Corporation (Bothell, WA) has already demonstrated modulators with drive voltages of 0.3-0.4 volts and > 20 GHz bandwidths. A strong driver for pushing toward 0.1 volt drive voltages is the potential for realizing gain in RF photonic applications. For resonant devices, bandwidth/sensitivity factors of greater than 20 GHz/V should be obtainable. The bandwidth and sensitivity gains to be realized for optical rectification (terahertz sources and detectors) should be dramatic and should facilitate the development of light-weight, compact terahertz systems including spectrometers. The integration of organic electro-optic materials with silicon photonics appears to be especially attractive affording the concentration of both optical and electric field due to reduced device dimensions. The smaller dimensions of such device structures may permit new processing techniques (layer-by-layer deposition and crosslinking of self-assembling materials) to be effectively implemented.

The importance of organic electro-optic materials does not lie in simple replacement of inorganic electro-optic materials in simple device structures such as Mach Zehnder interferometers but rather in the stimulation of new applications and device concepts. A significant opportunity for organic electro-optic materials is to facilitate the production of highly integrated electronic/photonic platforms (chipscale integration and higher). The integration of organic EO materials with silicon photonics is particularly attractive and provides a route to utilization of the tremendous resource of existing CMOS foundries.

While significant molecular, supramolecular, and device engineering challenges exist, the field of organic electro-optic materials appears to be entering an exciting new era that will likely see dramatic improvement in materials properties and device performance. The lessons learned in electro-optics are likely to be relevant to the engineering of improved properties for other organic electroactive materials and device applications (electronic, photovoltaic, photorefractive, and light emitting).

REFERENCES

1. Liao, L., B. E. Eichinger, K. A. Firestone, M. Haller, J. Luo, W. Kaminsky, J. B. Benedict, P. J. Reid, A. K-Y. Jen, L. R. Dalton, and B. H. Robinson, "Systematic study of the structure-property relationship of a series of ferrocenyl nonlinear optical chromophores", *J. Am. Chem. Soc*. **127**, 2758-2766 (2005).
2. Ishorn, C. M., A. Lerlercq, F. D. Vila, L. R. Dalton, J. L. Bredas, B. E. Eichinger, and B. H. Robinson, "Comparison of static first hyperpolarizabilities calculated with various quantum mechanical methods," *J. Phys. Chem. A* **111**, 1319-1327 (2007).
3. Jang, S. H., J. Luo, N. M. Tucker, A. Leclercq, E. Zojer, M. A. Haller, T. D. Kim, J. W. Kang, K. Firestone, D. Bale, D. Lao, J. B. Benedict, D. Cohen, W. Kaminsky, B. Kahr, J. L. Bredas, P. Reid, L. R. Dalton, and A. K. Y. Jen, "Pyrroline chromophores for electro-optics," *Chem. Mater*. **18**, 2983-2998 (2006).
4. Kinnibrugh, T., S. Bhattacharjee, P. Sullivan, C. Isborn, B. H. Robinson, and B. E. Eichinger, "Influence of isomerization on nonlinear optical properties of molecules," *J. Phys. Chem. B* **110**, 13512-13522 (2006).
5. Davidson, E. R., B. E. Eichinger and B.H. Robinson, "Hyperpolarizability: calibration of theoretical methods for chloroform, water, acetonitrile, and p-nitroaniline," *Opt. Mater.* **29**, 360-364 (2006).
6. Isborn, C. S., and B. H. Robinson, "*Ab initio* diradical/zwiterionic polarizabilities and hyperpolarizabilities in twisted diradicals," *J. Phys. Chem. A* **110**, 7189-7196 (2006).
7. Kang, H., A. Facchetti, H. Jiang, E. Cariati, S. Righetto, R. Ugo, C. Zuccacccia, A. Macchioni, C. L. Stern, Z. Liu, S. T. Ho, E. C. Brown, M. A. Ratner, and T. J. Marks, "Ultralarge hyperpolarizability twisted π-electron system electro-optic chromophores: Synthesis, solid-state and solution-phase structural characteristics, electronic structures, linear and nonlinear optical properties, and computational studies," *J. Am. Chem. Soc*. **129**, 3267-3286 (2007).
8. Wang, Y., "Theoretical design of molecular photonic materials," Ph.D. thesis, Royal Institute of Technology, Stockholm, Sweden, 2007.
9. Wang, C. K., Y. H. Wang, Y. Su, and Y. Luo, "Solvent dependence of solvatochromic shifts and the first hyperpolarizability of para-nitroaniline: A nonmonotonic behavior," *J. Chem. Phys*. **119**, 4409-4412 (2003).
10. Ando, S., T. Fujigaya, and M. Ueda, "Density functional theory calculation of photoabsorption spectra of organic molecules in the vacuum ultraviolet region," *Jpn. J. Appl. Phys*. **41**, L105-L108 (2002).
11. Dalton, L. R., A. W. Harper, and B. H. Robinson, "The role of London forces in defining noncentrosymmetric order of high dipole moment-high hyperpolarizability chromophores in electrically poled polymeric thin films," *Proc. Natl. Acad. Sci. USA* **94**, 4842-4847 (1997).

12. Dalton, L. R., B. H. Robinson, A. K. Y. Jen, W. H. Steier, and R. Nielsen "Systematic development of high bandwidth, low drive voltage organic electro-optic devices and their applications," *Opt. Mater*. **21**, 19-28 (2003).
13. Nielsen, R. D., H. L. Rommel, and B. H. Robinson, "Simulation of the loading parameter in organic nonlinear optical materials," *J. Phys. Chem. B* **108**, 8659-8667 (2004).
14. Piekara, A., "A theory of electric polarization, electro-optical Kerr effect and electric saturation in liquids and solutions," *Proc. Roy. Soc. Lon. A* **172**, 360-383 (1939).
15. Kim, W. K., and L. M. Hayden, "Fully atomistic modeling of an electric field poled guest-host nonlinear optical polymer," *J. Chem. Phys*. **111**, 5212-5222 (1999).
16. Leahy-Hoppa, M. R., P. D. Cunningham, J. A. French, and L. M. Hayden, "Atomistic molecular modeling of the effect of chromophore concentration on the electro-optic coefficient in nonlinear optical polymers," *J Phys Chem A* **110**, 5792-5797 (2006).
17. Makowska-Janusik, M., H. Reis, M. G. Papadopoulos, I. G. Economou, and N. Zacharopoulos, "Molecular dynamics simulations of electric field poled nonlinear optical chromophores incorporated in a polymer matrix," *J. Phys. Chem. B* **108**, 588-596 (2004).
18. Robinson, B. H., and L. R. Dalton, "Monte Carlo statistical mechanical simulations of the competition of intermolecular electrostatic and poling field interactions in defining macroscopic electro-optic activity for organic chromophore/polymer materials," *J. Phys. Chem*. **104**, 4785-4795 (2000).
19. Dalton, L. R., A. K. Y. Jen, P. Sullivan, B. Eichinger, B. H. Robinson, and A. Chen, "Theoretically-inspired rational design of electro-optic materials," *Nonlinear Optics and Quantum Optics*, **35**, 1-19 (2006).
20. Rommel, H. L., and B. H. Robinson, "Orientation of electro-optic chromophores under poling conditions: A spheroidal model," *J. Phys. Chem. B* submitted.
21. Rommel, H. L., "Determining the order parameters of organic nonlinear optical chromophores by Monte Carlo methods," Ph.D. Thesis, University of Washington, Seattle, USA, 2007.
22. Firestone, K. A., D. Bale, Y. Liao, D. M. Casmier, O. Clot, L. R. Dalton, and P. J. Reid, "Frequency-agile Hyper-Rayleigh Scattering studies of electro-optic chromophores," *Proc. SPIE*, **5935**, 59350P1-9 (2005).
23. Ostinelli, O., "Solvent dependence of microscopic optical nonlinearities of the bithiophene molecule CC172 and investigation of poling processes for polyimide AM3 148.02," M.S. Thesis, ETH, Zurich, Switzerland, 2000.
24. EFISH measurements were carried out by Denise Bale in the laboratory of Professor P. Gunter, ETH, Zurich, Switzerland in 2006. A detailed account of these measurements will be published elsewhere.
25. Teng, C. C., and H. T. Man, "Simple reflection technique for measuring the electro-optic coefficient of poled polymers," *Appl. Phys. Lett.* **56**, 1734-1736 (1990).

26. Sullivan, P. A., "Theory guided design and molecular engineering of organic materials for enhanced second-order nonlinear optical properties," Ph.D. Thesis, University of Washington, Seattle, WA, USA, 2006.
27. Chen, A., V. Chuyanov, S. Garner, W. H. Steier, L. R. Dalton, "Modified attenuated total reflection for the fast and routine electrooptic measurements of nonlinear optical polymer thin films," In *Organic Thin Films for Photonic Applications*, *vol. 14*, OSA Technical Digest Series (Optical Society of America, Washington DC, 1997) pp. 158-9; this instrument has been further modified by incorporation of a rutile prism permitting measurements to be carried out at both 1.3 and 1.55 microns and facilitating the measurement of both r_{33} and r_{13}.
28. Chen, A., V. Chuyanov, H. Zhang, S. Garner, W. H. Steier, J. Chen, J. Zhu, M. He, S. S. H. Mao, and L. R. Dalton, "Demonstration of the full potential of second order nonlinear optic polymers for electrooptic modulation using a high μβ chromophore and a constant bias field," *Optics Lett.* **23**, 478-480 (1998).
29. Bhatambrekar, N. P., L. R. Dalton, J. Luo, A. K. Y. Jen, and A. Chen, "Third order nonlinearity contribution to electro-optic activity in polymer materials in a constant DC bias field," *Appl. Phys. Lett.* **88**, 041115-1-3 (2005).
30. Rabiei, P., W. H. Steier, C. Zhang, and L. R. Dalton, "Polymer micro-ring filters and modulators," *J. Lightwave Technology* **20**, 1968-1975 (2002).
31. Baehr-Jones, T., M. Hochberg, G. Wang, R. Lawson, Y. Liao, P. A. Sullivan, L. R. Dalton, A. K. Y. Jen, and A. Scherer, "Optical modulation and detection in slotted silicon waveguides," *Optics Express* **13**, 5216-5226 (2005).
32. Hammond S., "Molecular and nanoscale engineering for enhanced order in organic electro-optic materials," Ph.D. Thesis, University of Washington, Seattle, WA, USA, 2007.
33. Sullivan, P. A., H. Rommel, Y. Liao, B. C. Olbricht, A. J. P. Akelaitis, K. A. Firestone, J. W. Kang, J. Luo, D. H. Choi, B. E. Eichinger, P. J. Reid, A. Chen, A. K. Y. Jen, B. H. Robinson, and L. R. Dalton, "Theory guided design and synthesis of multi-chromophore dendrimers and computational investigation of the origins of their improved electro-optic activity," *J. Amer. Chem. Soc.* 129, 7523-7530 (2007).
34. Sullivan, P. A., B. C. Olbricht, and L. R. Dalton, "Polarized absorption spectroscopy for the measurement of $\langle P_2 \rangle$ and correlation with measurement of $\langle \cos^3\theta \rangle$ by electro-optic techniques," *Appl. Phys. Lett.* submitted.
35. Sullivan, P. A., A. J. P. Akelaitis, S. K. Lee, G. McGrew, S. K. Lee, D. H. Choi, and L. R. Dalton, "Novel dendritic chromophores for electro-optics: Influence of binding mode and attachment flexibility on EO behavior," *Chem. Mater*. **18**, 344-351 (2006).
36. Sullivan, P. A., B. C. Olbricht, A. J. P. Akelaitis, A. A. Mistry, Y. Liao, and L. R. Dalton, "Tri-component Diels-Alder polymerized dendrimer glass exhibiting large, thermally stable, electro-optic activity," *J. Mater. Chem*. in press (2007).

37. Barto. R., Jr., P. V. Bedworth, C. W. Frank, S. Ermer, and R. E. Taylor, "Near-infrared optical-absorption behavior in high-beta nonlinear optical chromophore-polymer guest-host materials. II. Dye spacer length effects in an amorphous polycarbonate copolymer host," *J. Chem. Phys*. **122**, 234907 1-14 (2005).
38. Barto, R., Jr., C. W. Frank, P. V. Bedworth, S. Ermer, and R. E. Taylor, "Near-infrared optical absorption behavior in high-β nonlinear optical chromophore-polymer guest-host materials. 1. Continuum dielectric effects in polycarbonate hosts," *J. Phys. Chem. B* **108**, 8702-8715 (2004).
39. Kim, T. D., J. W. Kang, J. Luo, S. H. Jang, J. W. Ka, N. Tucker, J. B. Benedict, L. R. Dalton, T. Gray, R. M. Overney, D. H. Park, W. N. Herman and A. K.-Y. Jen, "Ultralarge and thermally stable electro-optic activities from supramolecular self-assembled molecular glasses," *J. Am. Chem, Soc*. **129**, 488-489 (2007).
40. Kim, T. D., Z. Shi, J. Luo, S. H. Jang, Y. J. Cheng, X. Zhou, S. Huang, L. R. Dalton, W. Herman, and A. K. Y. Jen, "New paradigm for ultrahigh electro-optic activity: Through supramolecular self-assembly and novel lattice hardening," *Proc. SPIE* **6470**, 64700D1-14 (2007).
41. Dalton, L. R., B. H. Robinson, A. K. Y. Jen, P. Reid, B. Eichinger, P. Sullivan, A. Akelaitis, D. Bale, M. Haller, J. Luo, S. Liu, Y. Liao, K. Firestone, N. Bhatambrekar, S. Bhattacharjee, J. Sinness, S. Hammond, N. Buker, R. Snoeberger, M. Lingwood, H. Rommel, J. Amend, S. H. Jang, A. Chen, and W. Steier, "Acentric lattice electro-optic materials by rational design," *Proc. SPIE*, **5912**, 43-54 (2005).
42. Pereverzev, Y. V., O. V. Prezhdo, and L. R. Dalton, "Macroscopic order and electro-optic response of dipolar chromophore-polymer materials," *Chem. Phys. Chem*. **5**, 1-11 (2004).
43. Natansohn, A., and P. Rochon, "Photoinduced motions in azo-containing polymers," *Chem. Rev*. **102**, 4139-4175 (2002).
44. Delaire, J. A., and K. Nakatani, "Linear and nonlinear optical properties of photochromic molecules and materials," *Chem. Rev*. **100**, 1817-1845 (2000).
45. Grote, J. S., J. S. Zetts, C. H. Zhang, R. L. Nelson, L. R. Dalton, F. K. Hopkins, and W. H. Steier, "Conductive Cladding Layers for Electrode Poled Nonlinear Optic Polymer Electro-Optics," *Proc. SPIE* **4114**, 101-109 (2000).
46. Grote, J. G., J. S. Zetts, R. L. Nelson, F. K. Hopkins, L. R. Dalton, C. Zhang, and W. H. Steier, "Effect of Conductivity and Dielectric Constant on the Modulation Voltage for Optoelectronic Devices Based on Nonlinear Optical Polymers", *Opt. Eng*. **40**, 2464-2473 (2001).
47. Grote, J. G., J. S. Zetts, R. L. Nelson, F. K. Hopkins, J. B. Huddleston, P. P. Yaney, C. H. Zhang, W. H. Steier, M.-C. Oh, H. R. Fetterman, A. K. Jen, and L. R. Dalton, "Advancements in Conductive Cladding Materials for Nonlinear-Optic-Polymer-Based Optoelectronic Devices," *Proc. SPIE* **4470**, 10-19 (2001).
48. Grote, J. G., J. S. Zetts, R. L. Nelson, F. K. Hopkins, P. P. Yaney, C. Zhang, W. H. Steier, M. C. Oh, H. R. Fetterman, A. K. Y. Jen, and L. R. Dalton,

"Conductive cladding materials for nonlinear optic polymer based opto-electronic devices," *Proc. GOMAC 2002* 161-165 (2002).
49. Leovich, M., P. P. Yaney, C. H. Zhang, W. H. Steier, M.-O. Oh, H. R. Fetterman, A. K. Y. Jen, L. R. Dalton, J. G. Grote, R. L. Nelson, J. S. Zetts, and F. K. Hopkins, "Optimized cladding materials for nonlinear-optic polymer-based devices," *Proc. SPIE* **4652**, 97-103 (2002).
50. Hagen, J. A., J. G. Grote, J. S. Zetts, D. E. Diggs, R. L. Nelson, F. K. Hopkins, P. P. Yaney, A. K. Jen, and L. R. Dalton, "Effects of the electric field poling procedure on electro-optic coefficient for guest-host nonlinear optic polymers," *Proc. SPIE* **5724**, 217-223 (2005).
51. Enami, Y., C. T. DeRose, C. Loychik, D. Mathine, R. A. Norwood, J. Luo, A. K. Y. Jen, and N. Peyghambarian, "Low half-wave voltage and high electro-optic effect in hybrid polymer/sol-gel waveguide modulators," *Appl. Phys. Lett.* **89**, 143506 1-3 (2006).
52. DeRose, C. T., Y. Enami, C. Loychik, R. A. Norwood, D. Mathine, M. Fallahi, N. Peyghambarian, J. D. Luo, A. K. Y. Jen, M. Kathaperumal, and M. Yamamoto, "Pockel's coefficient enhancement of poled electro-optic polymers with a hybrid organic-inorganic sol-gel cladding layer," *Appl. Phys. Lett.* **89**, 131102 1-3 (2006).
53. Gan, H., H. Zhang, C. T. DeRose, R. A. Norwood, N. Peyhambarian, M. Fallahi, J. Luo, B. Chen, and A. K. Y. Jen, "Low drive voltage Fabry-Perot etalon device tunable filters using poled hybrid sol-gel materials," *Appl. Phys. Lett.* **89**, 041127 1-3 (2006).
54. Enami, Y., C. T. DeRose, D. Mathine, C. Loychik, C. Greenlee, R. A. Norwood, T. D. Kim, J. Luo, Y. Tian, A. K. Y. Jen, and N. Peyghambarian, "Hybrid polymer/sol-gel waveguide modulators with exceptionally large electro-optic coefficients," *Nature Photonics* **1**, 180-185 (2007).
55. Song, R., A. Yick, and W. H. Steier, "Conductivity-dependency-free in-plane poling for Mach-Zehnder modulator with highly conductive electro-optic polymer," *Appl. Phys. Lett.* **90**, 191103 1-3 (2007).
56. Xu, G., J. Ma, Z. Liu, B. Liu, S. T. Ho, P. Zhu, L. Wang, Y. Yang, T. J. Marks, J. Luo, N. Tucker, and A. K. Y. Jen, "Low-voltage organic electro-optic modulators using transparent conducting oxides as electrodes," *Optics Express* **13**, 7380-7385 (2005).
57. Wang, L., Y. Yang, and T. J. Marks, "Near-infrared transparent electrodes for precision Teng-Man electro-optic measurements. In_2O_3 thin film electrodes with tunable near-infrared transparency," *Appl. Phys. Lett.* **87**, 161107 1-3 (2005).
58. Dalton, L. R., A. W. Harper, R. Ghosn, W. H. Steier, M. Ziari, H. Fetterman, Y. Shi, R. Mustacich, A. K.-Y. Jen, and K. J. Shea, "Synthesis and processing of improved second order nonlinear optical materials for applications in photonics," *Chem. Mater.* **7**, 1060-1081 (1995).
59. Mao, S. S. H., Y. Ra, L. Guo, C. Zhang, L. R. Dalton, A. Chen, S. Garner, and W. H. Steier, "Progress towards device-quality second-order nonlinear optical materials: 1. Influence of composition and processing conditions on

nonlinearity, temporal stability and optical loss," *Chem. Mater.* **10**, 146-155 (1998).
60. Haller, M., J. Luo, Hongxian Li, T. D. Kim, Y. Liao, B. Robinson, L. R. Dalton, and A. K. Y. Jen, "A novel lattice-hardening process to achieve highly efficient and thermally stable nonlinear optical polymers," *Macromolecules* **37**, 688-690 (2004).
61. Tucker, N., H. Li, H. Tang, L. R. Dalton, Y. Liao, B. H. Robinson, A. K. Jen, J. Luo, S. Liu, M. Haller, J. Kang, T. Kim, S. Jang and B. Chen, "Recent progress in developing highly efficient and thermally stable nonlinear optical polymers for electro-optics," *Proc. SPIE*, **5351**, 36-43 (2004).
62. Zhang, C., H. Zhang, M. Oh, L. Dalton, and W. Steier, "What the ultimate polymeric electro-optic materials will be: Guest-host, crosslinked, or side-chain," *Proc. SPIE* **4991**, 537-551 (2003).
63. Jin, D., T. Londergan, D. Huang, N. Wolf, S. Condon, D. Tolstedt, H. Guan, S. Cong, E. Johnson, and R. Dinu, "Achieving large electro-optic response: DH-type chromophores in both crosslinked systems and linear high Tg systems," *Proc. SPIE* **5351**, 44-56 (2004).
64. Luo, J., M. Haller, H. Ma, S. Liu, T. D. Kim, Y. Tian, B. Chen, S. H. Jang, L. R. Dalton, and A. K. Y. Jen, "Nanoscale architectural control and macromolecular engineering of nonlinear optical dendrimers and polymers for electro-optics," *J. Phys. Chem. B* **108**, 8523-8530 (2004).
65. Suresh, S., S. Chen, C. M. Topping, J. M. Ballato, and D. W. Smith, Jr., "Novel perfluorocyclo-butyl (PFCB) polymers containing isophorone derived chromophore for electro-optic [EO] applications," *Proc. SPIE* **4991**, 530-536 (2003).
66. P. A. Sullivan, P. A., A. J. P. Akelaitis, S. K. Lee, G. McGrew, S. K. Lee, D. H. Choi, and L. R. Dalton, ""Novel dendritic chromophores for electro-optics: Influence of binding mode and attachment flexibility on EO behavior," *Chem. Mater*. **18**, 344-351 (2006).
67. Lindsay, G. A., A. J. Guenthner, M. E. Wright, M. Sanghadasa, and P. R. Ashley, "Long-term alignment stability of CLD and FTC chromophores in polycarbonate and polyimide poled glassy films at elevated temperatures," *Macromolecules*, in press (2007).
68. Zhang, C., L. R. Dalton, M. C. Oh, H. Zhang, and W. H. Steier, "Low V_{π} electrooptic modulators from CLD-1: Chromophore design and synthesis, materials processing, and characterization," *Chem. Mater*. **13**, 3043-3050 (2001).
69. Zhang, Q., M. Canva, and G. Stegeman, "Wavelength dependence of 4-dimethylamino-4'-nitrostilbene polymer thin film photodegradation," *Appl. Phys. Lett*. **73**, 912-914 (1998).
70. Galvan-Gonzalez, A., M. Canva, G. I. Stegeman, R. J. Twieg, T. C. Kowalczyk, and H. S. Lackritz, "Effect of temperature and atmospheric environment on the photodegradation of some Disperse Red 1 type polymers," *Opt. Lett*. **24**, 1741-1743 (1999).

71. Galvan-Gonzalez, A., M. Canva, G. I. Stegeman, R. J. Twieg, K. P. Chang, T. C. Kowalczyk, X. Q. Zhang, H. S. Lackritz, S. Marder, and S. Thayumanavan, "Systematic behavior of electro-optic chromophore photostability," *Opt. Lett.* **25**, 332-334 (2000).
72. Galvan-Gonzalez, A., M. Canva, G. I. Stegeman, L. Sukhomilinova, R. J. Twieg, K. P. Chang, T. C. Kowalczyk, and H. S. Lackritz, "Photodegradation of azobenzene nonlinear optical chromophores: The influence of structure and environment," *J. Opt. Soc. Am. B* **17**, 1992-2000 (2000).
73. DeRosa, M. E., M. He, J. S. Cites, S. M. Garner, and Y. R. Tang, "Photostability of high μβ electro-optic chromophores at 1550 nm," *J. Phys. Chem. B* **108**, 8725-8730 (2004).
74. He, M., T. Leslie, S. Garner, M. E. DeRosa, and J. Cites, "Synthesis of new electrooptic chromophores and their structure-property relationship," *J. Phys. Chem. B* **108**, 8731-8736 (2004).
75. Rezzonico, D., M. Jazbinsek, C. Bosshard, P. Gunter, D. H. Bale, Y. Liao, L. R. Dalton, and P. J. Reid, "Photostability studies of π-conjugated chromophores with resonant and nonresonant excitations," *J. Opt. Soc. B* in press.
76. Taylor, E. W., J. E. Nichter, F. D. Nash, F. Haas, A. A. Szep, R. J. Michalak, B. M. Flusche, P. R. Cook, T. A. McEwen, B. F. McKeon, P. M. Payson, G. A. Brost, A. R. Pirich, C. Castaneda, B. Tsap, and H. R. Fetterman, "Radiation resistance of electro-optic polymer-based modulators," *Appl. Phys. Lett*. **86**, 201122-1-3 (2005).
77. Song, H. C., M. C. Oh, S. W. Ahn, and W. H. Steier, "Flexible low-voltage electro-optic polymer modulators," *Appl. Phys. Lett.* **82**, 4432-4434 (2003).
78. Dalton, L. R., A. W. Harper, A. Ren, F. Wang, G. Todorova, J. Chen, C. Zhang, and M. Lee, "Polymeric electro-optic modulators: From chromophore design to integration with semiconductor VLSI electronics and silica fiber optics," *Ind. Eng. Chem. Res* **38**, 8-33 (1999).
79. Yariv, A., C. Zhang, L. R. Dalton, Y. Huang, and G. T. Paloczi, "Fabrication and replication of polymer integrated optical devices using electron-beam lithography and soft lithography," *J. Phys. Chem. B* **108**, 8006-8013 (2004).
80. Paloczi, G. T., Y. Huang, A. Yariv, J. Luo, A. Jen, "Replica-molded electro-optic polymer Mach-Zehnder modulator," *Appl. Phys. Lett.* **85**, 1662-1664 (2004).
81. Hochberg, M., T. Baehr-Jones, G. Wang, J. Parker, K. Harvard, J. Liu, B. Chen, Z. Shi, R. Lawson, P. Sullivan, A. K. Y. Jen, L. R. Dalton, and A. Scherer, "All optical modulator in silicon with terahertz bandwidth," *Nature Materials* **5**, 703-709 (2006).
82. Dalton, L. R., "Organic electro-optic materials," in *Conjugated Polymers: Processing and Applications* (eds. Skotheim, T. A., and J. R. Reynods), CRC Press, Boca Raton, FL, (2007), pp. 6-1 to 6-39.
83. Dalton, L. R., A. W. Harper, B. Wu, R. Ghosn, J. Laquindanum, Z. Liang, A. Hubbel, and C. Xu, "Polymeric electro-optic modulators: Materials synthesis and processing," *Adv. Mater.* **7**, 519-540 (1995).

84. Kim, J. H., L. Sun, C.-H. Jang, D. An, J. M. Taboada, Q. Zhou, X. Lu, R. T. Chen, X. Han, S. Tang, H. Zhang, W. H. Steier, A. Ren, and L. R. Dalton, "Polymeric waveguide beam deflector for electro-optic switching," *Proc SPIE* **4279**, 37-44 (2001).
85. Sun, L., J. Kim, C. Jang, D. An, X. Lu, Q. Zhou, J. M. Taboada, R. T. Chen, J. J. Maki, S. Tang, H. Zhang, W. H. Steier, C. Zhang, and L. R. Dalton, "Polymeric waveguide prism based electro-optic beam deflector," *Opt. Eng*. **40**, 1217-1222 (2001).
86. Rabiei, P., W. H. Steier, C. Zhang, and L. R. Dalton, "Polymer micro-ring filters and modulators," *J. Lightwave Technology* **20**, 1968-1975 (2002).
87. Baehr-Jones, T., M. Hochberg, G. Wang, R. Lawson, Y. Liao, P. A. Sullivan, L. R. Dalton, A. K. Y. Jen, and A. Scherer, "Optical modulation and detection in slotted silicon waveguides," *Optics Express* **13**, 5216-5226 (2005).
88. Michael Hochberg, M., T. Baehr-Jones, G. Wang, J. Huang, P. Sullivan, L. Dalton, and A. Scherer, "Toward a millivolt optical modulator with nano-slot waveguides", *Optical Express* **15**, 8401-8410 (2007).
89. Takayesu, J., M. Hochberg, T. Baehr-Jones, E. Chan, D. Koshniz, G. Wang, P. Sullivan, Y. Liao, J. Davies, L. Dalton, A. Scherer, and W. Krug, "Hybrid electro-optic microring resonator filters for use in VLSI applications," *J. Lightwave Technology* submitted.
90. Sinyukov, A. M., and L. M. Hayden, Efficient electrooptic polymers for THz applications, *J. Phys. Chem. B* **108**, 8515-8522 (2004).
91. Sinyukov, A. M., M. R. Leahy, L. M. Hayden, M. Haller, J. Luo, A. K. Y. Jen, and L. R. Dalton, "Resonance enhanced THz generation in electro-optic polymers near the absorption maximum," *Appl. Phys. Lett*. **85**, 5827-5829 (2004).
92. Dalton, L. R., "Nonlinear optical polymeric materials: From chromophore design to commercial applications," in *Advances in Polymer Science* **Vol 158** (Springer-Verlag, Heidelberg, 2001), pp. 1-86.
93. Dalton, L. R., "Novel Polymer-Based, High-Speed Electro-Optic Devices," *Proceedings 23rd European Conference on Optical Communications/14th International Conference on Integrated Optics and Optical Fibre Communication* (2003), vol. 2, pp. 346-9.
94. Bechtel, J. H., Y. Shi, H. Zhang, W. H. Steier, C. H. Zhang, and L. R. Dalton, "Low-driving-voltage electro-optic polymer modulators for advanced photonic applications," *Proc. SPIE* **4114**, 58-64 (2000).
95. Fetterman, H. R., D. H. Chang, H. Erlig, M. Oh, C. H. Zhang, W. H. Steier, and L. R. Dalton, "Photonic time-stretching of 102 GHz millimeter waves using 1.55 μm polymer electro-optic modulator," *Proc. SPIE* **4114**, 44-57 (2000).
96. Lee, S. S., A. H. Udupa, H. Erlig, H. Zhang, Y. Chang, C. Zhang, D.H. Chang, D. Bhattacharya, B. Tsap, W. H. Steier, L. R. Dalton, and H. R. Fetterman, "Demonstration of a photonically controlled RF phase shifter," *IEEE Microwave and Guided Wave Letters* **9**, 357-359 (1999).

97. A. Yacoubian, A., V. Chuyanov, S. M. Garner, W. H. Steier, A. S. Ren, and L. R. Dalton, "EO polymer-based integrated-optical acoustic spectrum analyzer," *IEEE J. Sel. Topics in Quantum Electronics* **6**, 810-816 (2000).
98. H. Sun, A. Pyajt, J. Luo, Z. Shi, S. Hau, A. K. Y. Jen, L. R. Dalton, and A. Chen, "All-dielectric electrooptic sensor based on a polymer microresonator coupled side-polished optical fiber," *IEEE Sensors Journal* **7**, 515-524 (2007).
99. Bhola, B., H. C. Song, H. Tazawa, and W. H. Steier, Polymer microresonator strain sensors, *IEEE Phot. Tech. Lett*. **17**, 867-870 (2005).

FIGURE CAPTIONS

Fig. 1. The evolution of electro-optic activity with time for materials used to fabricate prototype devices is shown. The star indicates the DARPA MORPH phase II goal. The rate of increase is greater than that predicted by a Moore's law plot.

Fig. 2. The structures of some common electro-optic chromophores are shown.

Fig. 3. Representative guest chromophore and chromophore-containing-host materials used to fabricate binary chromophore containing organic glasses are shown.

Fig. 4. Top. (a) A schematic diagram of a Teng-Man apparatus modified for *in-situ* monitoring of poling and relaxation of poling-induced order and for laser-assisted poling experiments is shown. Bottom. (b) A schematic diagram of an attenuated total reflection (ATR) apparatus for the measurement of all elements of the electro-optic tensor is shown.

Fig. 5. The frequency dependence of molecular first hyperpolarizability, β, is compared for density functional theory (dark dashed line) and two-level model (light dashed line) calculations.

Fig. 6. (a) The chemical structure of the PSLD-33 dendrimer is shown. (b) The pseudo-atomistic Monte Carlo representation of the PSLD-33 dendrimer is shown.

Fig. 7. Both theory and experiment suggest a linear dependence for the variation of electro-optic activity (r_{33}) with poling voltage (E_p). Data are shown for the PSLD-33 dendrimer.

Fig. 8. First principles theoretical data (open circles) and experimental data (solid circles) for PSLD-41 and PSLD-33 multi-chromophore-containing dendrimers are shown. Also shown are the experimental data (solid

diamonds) for the same chromophore in APC composite materials. Note that the maximum electro-optic activity for the CF3FTC/APC composite materials occurs at a number density of 2.5 x 10^{20} chromophores/cc; the electro-optic activity decreases at higher loading and phase separation starts to occur. Substantially higher loading is achieved for the multi-chromophore-containing dendrimer materials; the chromophores act as independent particles (note the linear dependence on number density). Also shown in this figure are the Monte Carlo theoretical results for the CF3FTC chromophore treated as a spherical object; this can be considered the optimum electro-optic activity for a single chromophore/polymer composite material.

Fig. 9. Experimental (dark solid circles) electro-optic (r_{33}/E_p) data are shown for binary chromophore organic glasses (BCOGs) formed by dissolving the YLD-124 chromophore into the PSLD-41 multi-chromophore-containing dendrimer (see Fig. 3). The course-grained MC calculation results are indicated by the dark solid line. The inset is a cartoon representation of one particularly favorable interaction configuration between the two chromophore components of the BCOG. Also shown in this figure is the experimental data for the neat dendrimers (PSLD-33 and PSLD-41).

Fig. 10. The theoretically-predicted variation of acentric order parameter with poling energy is shown as a function of the symmetry of the lattice in which the chromophore is embedded. Acentric order, and thus electro-optic activity, is predicted to increase in progressing from 3-D (Langevin) to 2-D (Bessel) to 1-D (Ising) symmetry. The straight line is the result predicted for independent particles (chromophores experiencing no intermolecular electrostatic interactions).

Fig. 11. A representative real-time result from a laser-assisted poling experiment is shown. The lower curve represents the temporal behavior of electro-optic activity measured using the Teng-Man apparatus of Fig. 4. The upper curve represents the variation of temperature (heating) with time. Note the dramatic increase in electro-optic activity when the polarized laser field is turned on. Systematic investigation of the dependence of the effect on laser power and temperature has been carried out.

Fig. 12. The variation of electro-optic activity, r_{33}, of a YLD-124/(DR1)-co-PMMA BCOG is shown as a function of electric poling voltage with and without laser-assisted poling.

Fig. 13. The variation of electro-optic activity, r_{33}, of a YLD-124/(DR1)-co-PMMA BCOG is shown as a function of chromophore number density with (triangles, solid line) and without (squares, dashed line) laser-assisted poling.

Fig. 14. The linear absorption spectra of YLD-124/(DR1)-co-PMMA BCOGs are shown as a function of YLD-124 concentration.

Fig. 15. The variation of current with temperature is shown for a crosslinked BCOG. The on-set of current flow indicates lattice softening and the movement of chromophores. This current flow could be due either to the diffusion of ionic impurities or to the on-set of variable ranging hopping of charge between the chromophores. Materials are typically purified to the point that no further change in current versus temperature curves are observed. Although ionic conductivity cannot be ruled out, it is our strong suspicion that the observed conductivity involves charge hopping among the chromophores.

Fig. 16. The variation of poling profiles with chromophore concentration is shown. The maximum achievable poling voltage is defined by the on-set of conductivity. Note that the rate of change of electro-optic activity with electric poling voltage together with the maximum achievable poling voltage define the maximum achievable electro-optic activity.

Fig. 17. (a) Cycloaddition crosslinking by reaction of a fluorovinyl either moiety to form cyclobutyl crosslinks is depicted. (b) Diels-Alder/Retro Diels Alder crosslinking is shown. (c) Representative diene and dienophiles are shown.

Fig. 18. The variation of electro-optic activity (measured using the *in situ* Teng Man apparatus of Fig. 4) with thermal ramping is shown. The material shown in this example is an uncrosslinked multi-chromophore-containing dendrimer (similar to the structures shown in Fig. 3 but with different spacer moieties).

Fig. 19. A schematic diagram of the apparatus used to define photostability is shown together with a typical kinetic trace. The experimental data is for a 25% FTC sample in APC.

Fig. 20. A micrograph (top) of a slotted ring resonator is shown together with electro-optic tuning of the bandpass notches (bottom). The middle figure slows the concentration of the optical field in the silicon waveguide slot where the organic electro-optic material is located.

AUTHOR BIOGRAPHIES

Larry R. Dalton is the George B. Kauffman Professor of Chemistry and Electrical Engineering and the Director of the National Science Foundation Science and Technology Center on Materials and Devices for Information Technology

Research at the University of Washington. He is currently a member of the Nanotechnology Technical Advisory Group of the Preisdent's Council of Advisors for Science and Technology, the Defense Science Board Advisory Group on Electronic Devices, and the NSF Mathematical and Physical Sciences Directorate Advisory Committee.

Philip A. Sullivan is currently a Research Associate in the Department of Chemistry at the University of Washington, Seattle. He received his B.S. degree in 2001 from Montana State University, Bozeman and his Ph.D. in 2006 from University of Washington, Seattle. He has coauthored more than 20 publications. His current research interests focus on organic materials for optoelectronic and sensor applications.

Denise H. Bale is currently a Ph.D. candidate in chemistry at the University of Washington. She received a B.S. (Honors) in chemistry from Western Washington University, Bellingham, WA (2002) and a M.S. in chemistry from the University of Washington, Seattle, WA (2004). Doctoral thesis work focuses on characterization of electro-optic materials including photostability and hyperpolarizability of chromophores through femtosecond, wavelength-agile hyper Rayleigh Scattering measurements.

Scott R. Hammond is a Research Associate at the University of Washington. He received his B.S. degree in chemistry with high honors from the University of California, Berkeley in 2001, and his Ph.D. in organic/materials chemistry and nanotechnology from the University of Washington, Seattle in 2007. He is coauthor on more than 10 journal articles. His research interests are in organic nanostructured materials with new or improved photonic and optoelectronic properties.

Benjamin C. Olbricht is a Ph.D. graduate student in the Department of Chemistry at the University of Washington, Seattle. He received his M.S. degree in Chemistry from the University of Washington in 2007 and a B.A. in Chemistry from Albion College in 2005. He is currently studying electro-optic materials including the processing of materials by laser-assisted-poling.

Harrison Rommel received his B.S. in Biochemistry from the University of New Mexico. He received his Ph.D. in Physical Chemistry from the University of Washington in 2007. His current research interests include investigation of the field-induced ordering of bulk organic NLO materials by Monte Carlo methods.

Bruce Eichinger is a Staff Scientist in the Department of Chemistry at the University of Washington. He received a B. Chem. from the University of Minnesota and Ph.D. from Stanford University. He came to his present position after working in the private sector for 13 years; prior to that time he served for 21 years on the chemistry faculty at the University of Washington. He has

published over 120 papers in the areas of polymer science and electro-optic materials. His current research is aimed at theoretical understanding and prediction of the electro-optic properties of molecules.

Bruce H. Robinson is Professor of Chemistry at the University of Washington and Associate Director of the NSF-STC on Materials and Devices for Information Technology Research. He received his B.S. in Chemistry form Princeton University and his Ph.D. in Chemistry from Vanderbilt University. His current research interests include biological magnetic resonance and the theory of intermolecular electrostatic interactions relevant to optimizing the performance of organic electro-optic materials.

FIGURES

Fig. 1

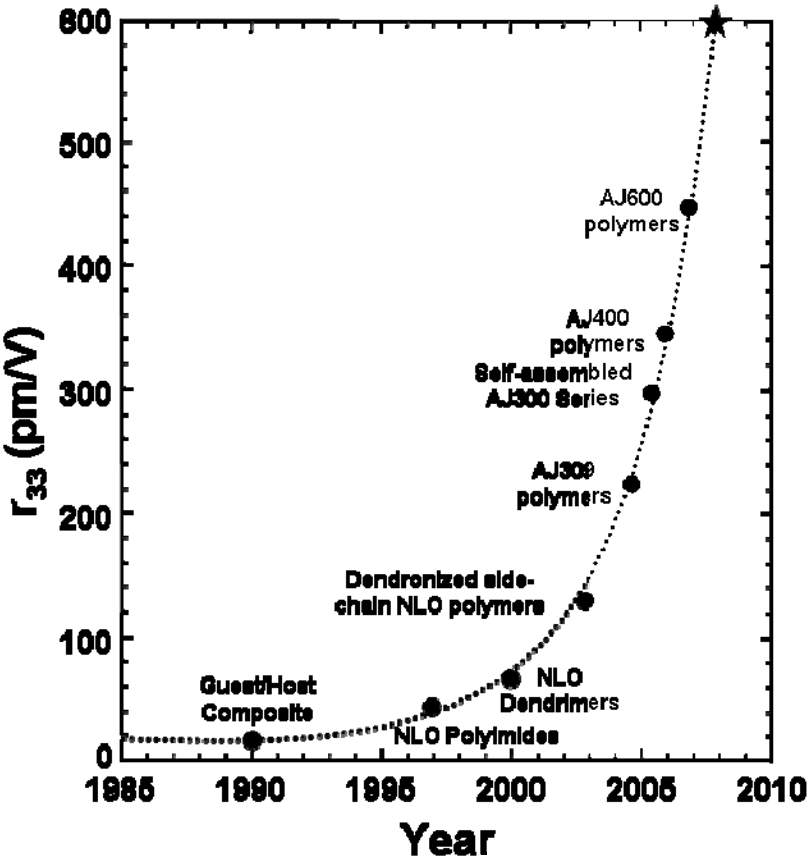
600
500
400
300
200
100
0
r_{33} (pm/V)
1985
1990
1995
2000
2005
2010
Year
AJ600 polymers
AJ400 polymers
Self-assembled AJ300 Series
AJ300 polymers
Dendronized side-chain NLO polymers
NLO Dendrimers
Guest/Host Composite
NLO Polyimides

Fig. 2

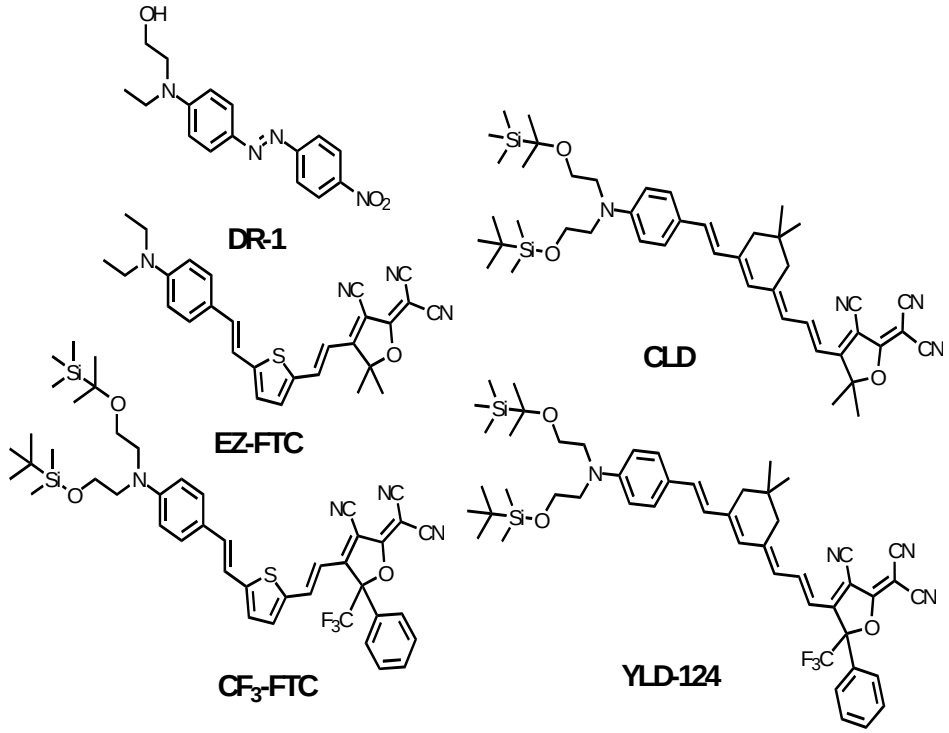

Fig. 3

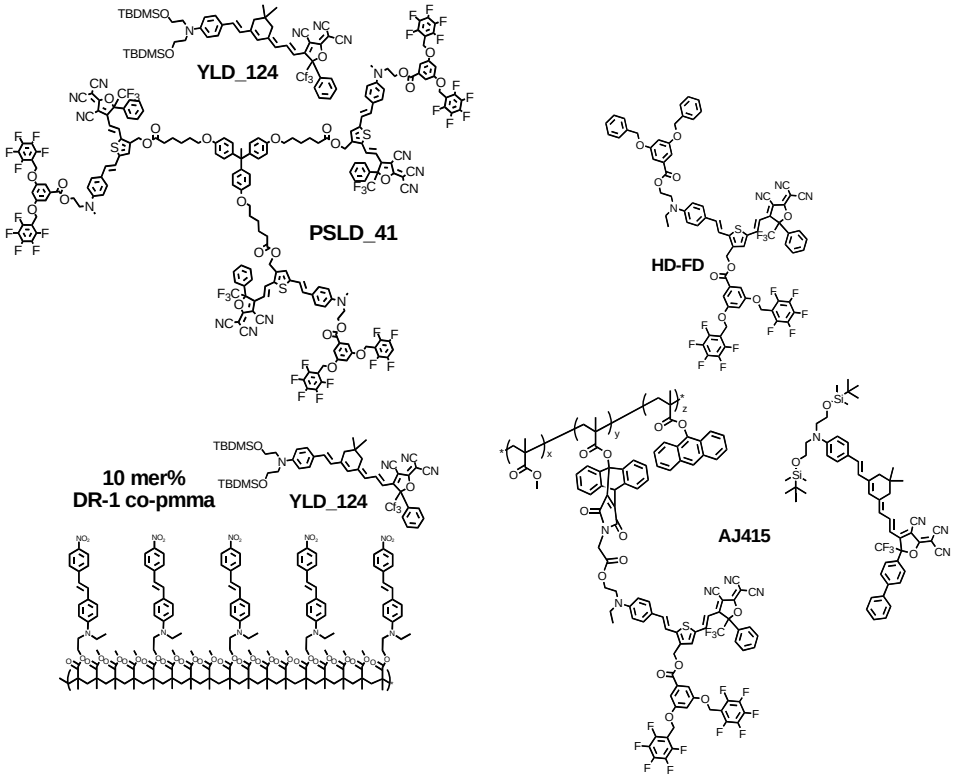

Fig. 4

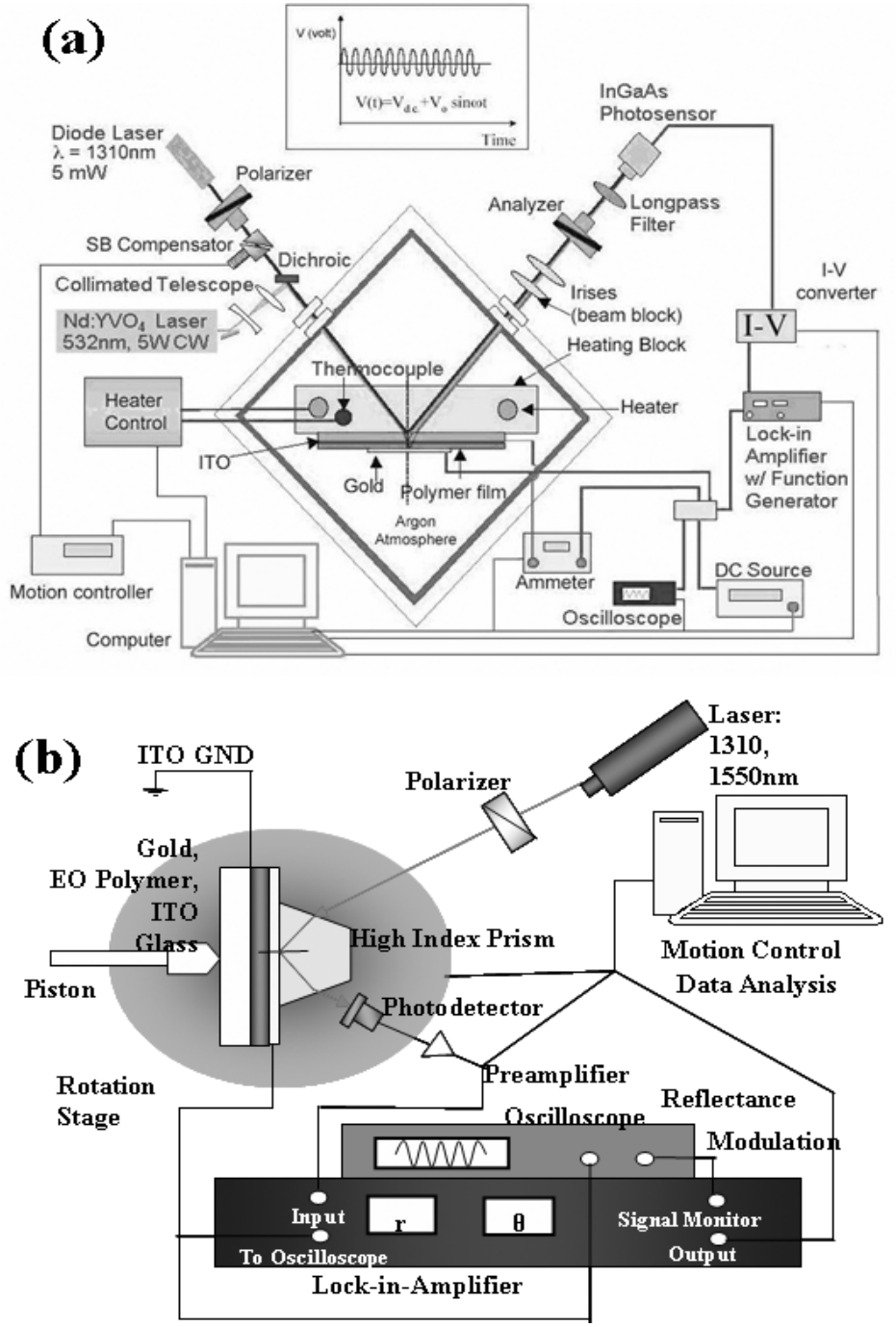
(a)
V (volt)
V(t)=V_dc+V_o sinωt
Time
InGaAs Photosensor
Diode Laser
λ = 1310nm
5 mW
Polarizer
Analyzer
Longpass Filter
SB Compensator
Dichroic
Collimated Telescope
Nd:YVO4 Laser
532nm, 5W CW
Irises (beam block)
I-V converter
I-V
Heating Block
Thermocouple
Heater Control
Heater
Lock-in Amplifier w/ Function Generator
ITO
Gold
Polymer film
Argon Atmosphere
Motion controller
Ammeter
DC Source
Oscilloscope
Computer
(b)
ITO GND
Laser: 1310, 1550nm
Polarizer
Gold, EO Polymer, ITO Glass
High Index Prism
Motion Control Data Analysis
Piston
Photodetector
Preamplifier
Rotation Stage
Reflectance
Oscilloscope
Modulation
Input
r
θ
Signal Monitor
To Oscilloscope
Output
Lock-in-Amplifier

Fig. 5

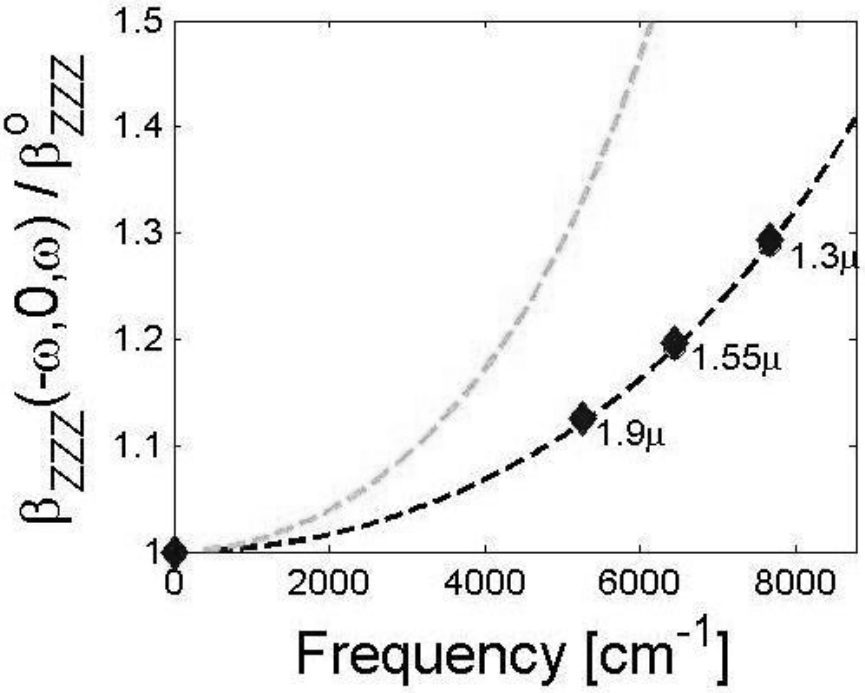
1.5
1.4
1.3
1.2
1.1
1
0
2000
4000
6000
8000
1.3μ
1.55μ
1.9μ
$\beta_{ZZZ}(-\omega,0,\omega) / \beta^{o}_{ZZZ}$
Frequency [cm^{-1}]

Fig. 6

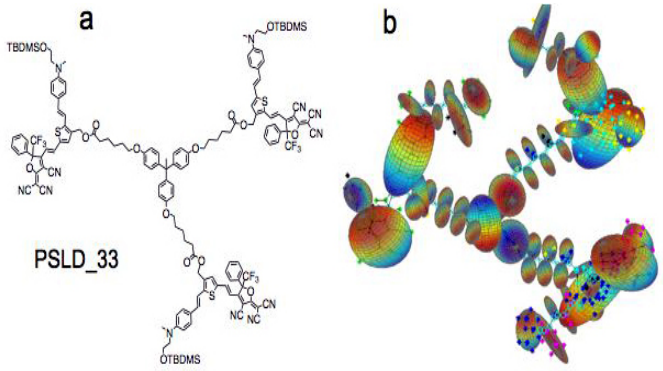

Fig. 7

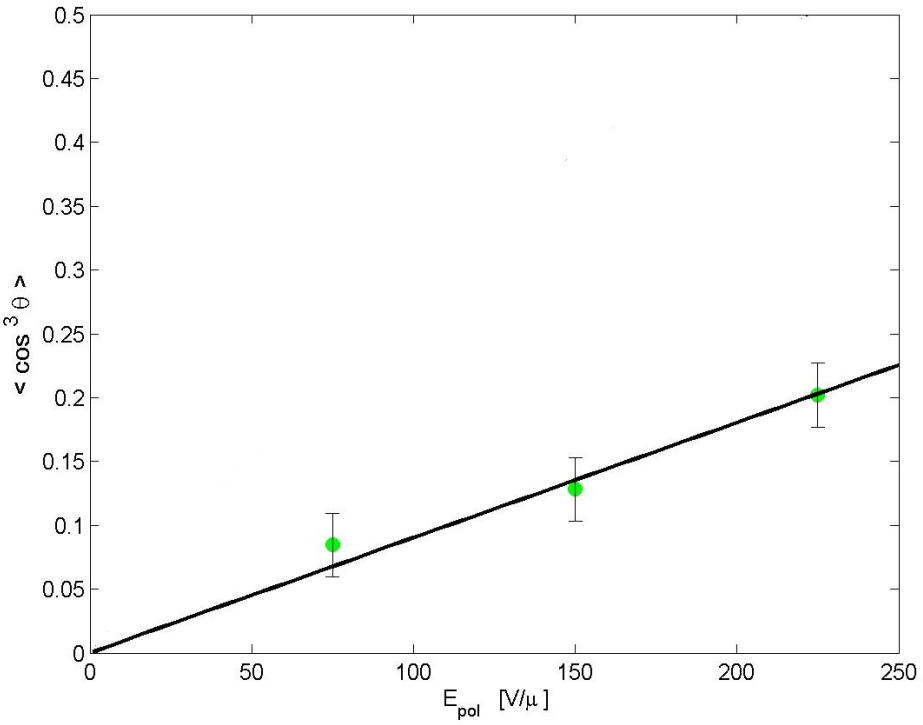
0.5
0.45
0.4
0.35
0.3
0.25
0.2
0.15
0.1
0.05
0
< cos 3 θ >
0
50
100
150
200
250
E pol [V/μ]

Fig. 8

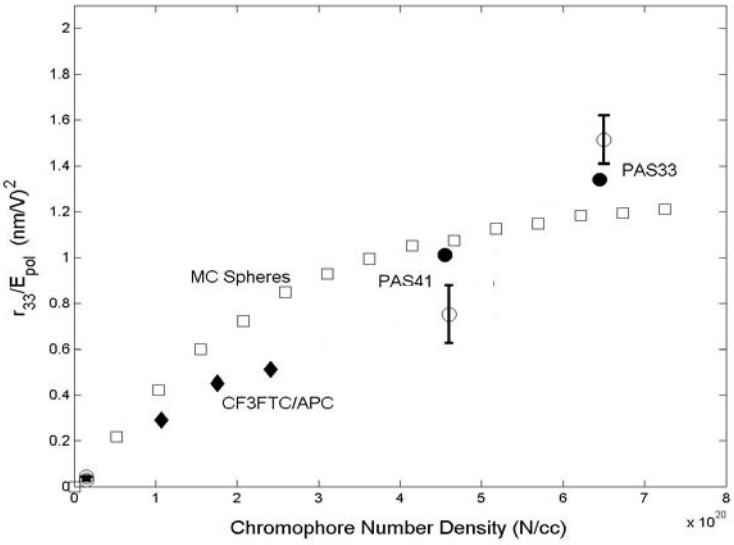
r_{33}/E_{pol} (nm/V)^2
Chromophore Number Density (N/cc)
x 10^{20}
MC Spheres
PAS41
PAS33
CF3FTC/APC
0
0.2
0.4
0.6
0.8
1
1.2
1.4
1.6
1.8
2
0
1
2
3
4
5
6
7
8

Fig. 9

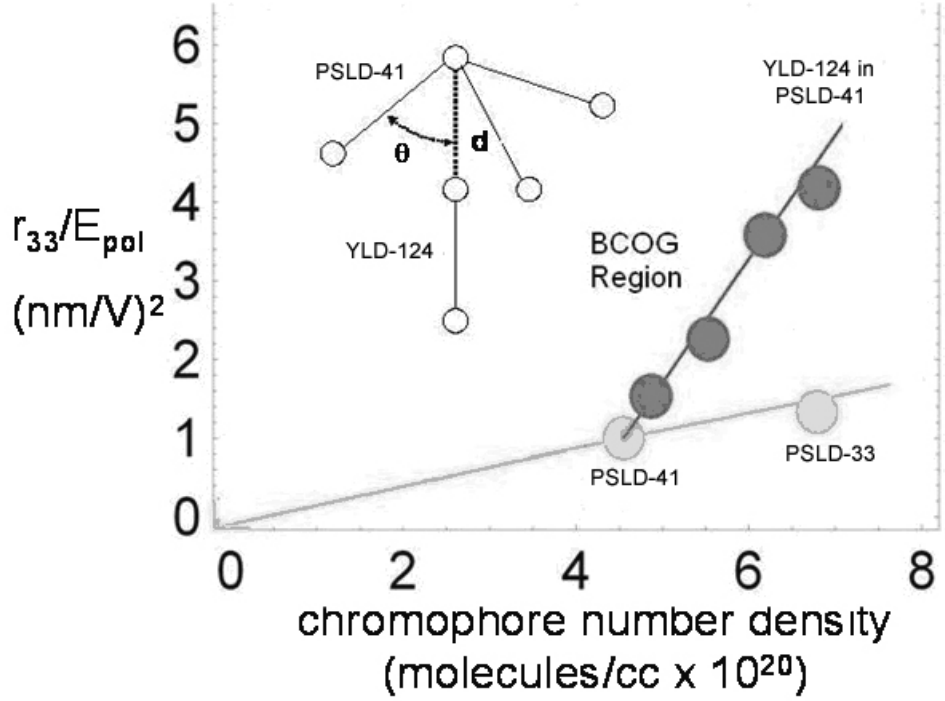
PSLD-41
θ
d
YLD-124
YLD-124 in
PSLD-41
BCOG
Region
PSLD-41
PSLD-33
r_{33}/E_{pol}
$(nm/V)^2$
0
1
2
3
4
5
6
0
2
4
6
8
chromophore number density
(molecules/cc x 10^{20})

Fig. 10

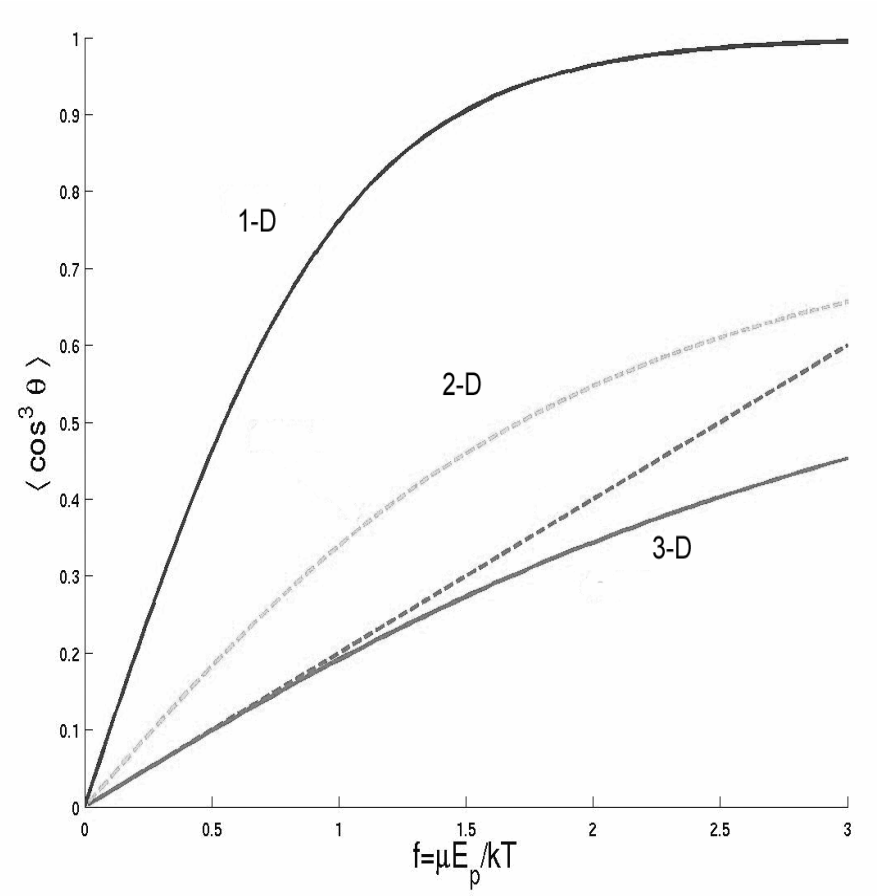

Fig. 11

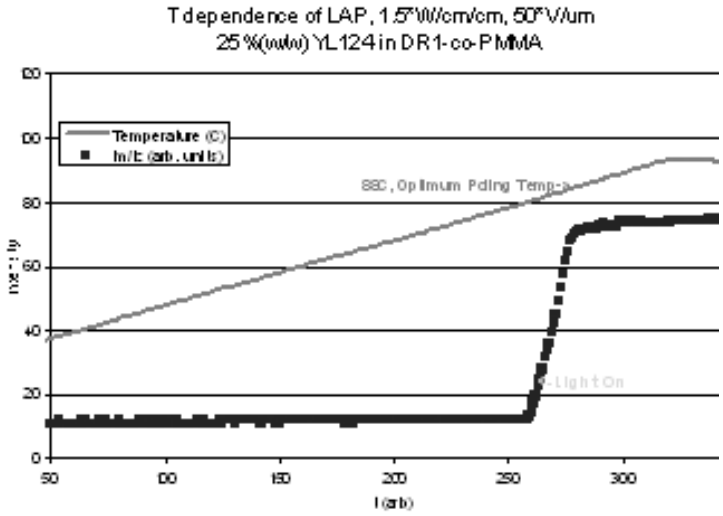
T dependence of LAP, 1.5*W/cm/cm, 50*V/um
25%(w/w) YL124 in DR1-co-PMMA
Temperature (C)
SSC, Optimum Poling Temp
Light On
I (arb)

Fig. 12

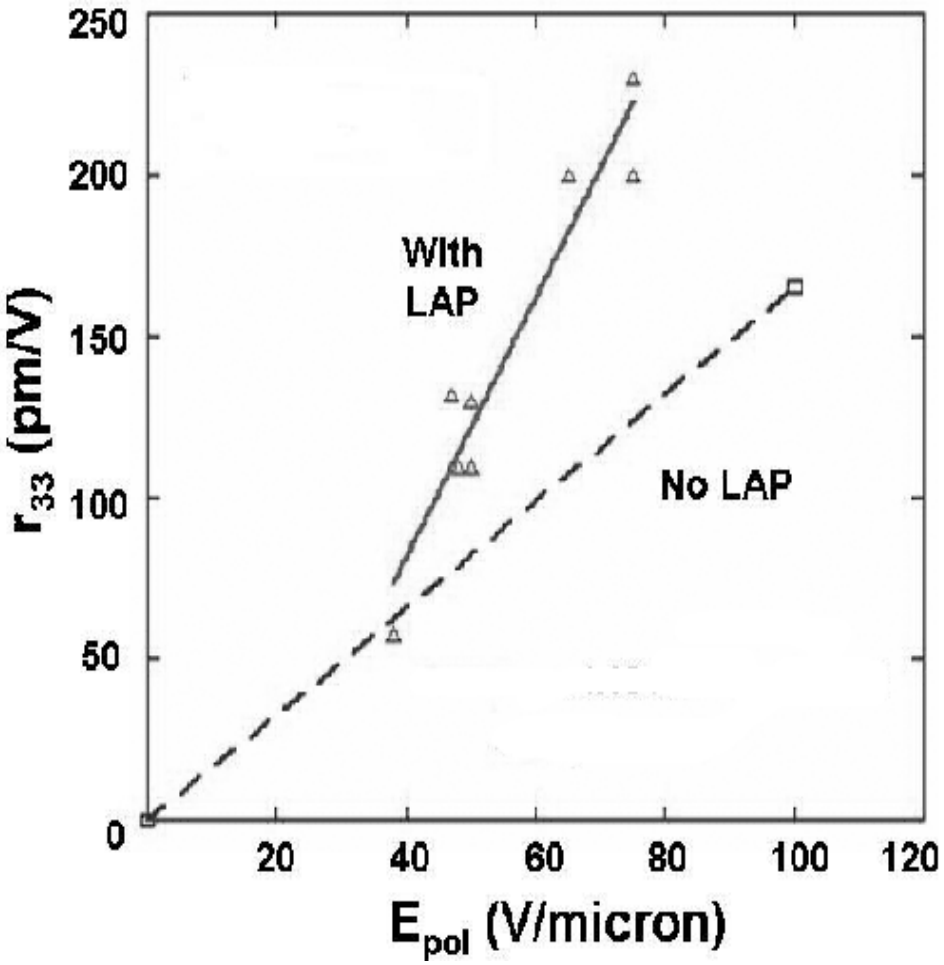
250
200
150
100
50
0
r_{33} (pm/V)
With
LAP
No LAP
20
40
60
80
100
120
E_{pol} (V/micron)

Fig. 13

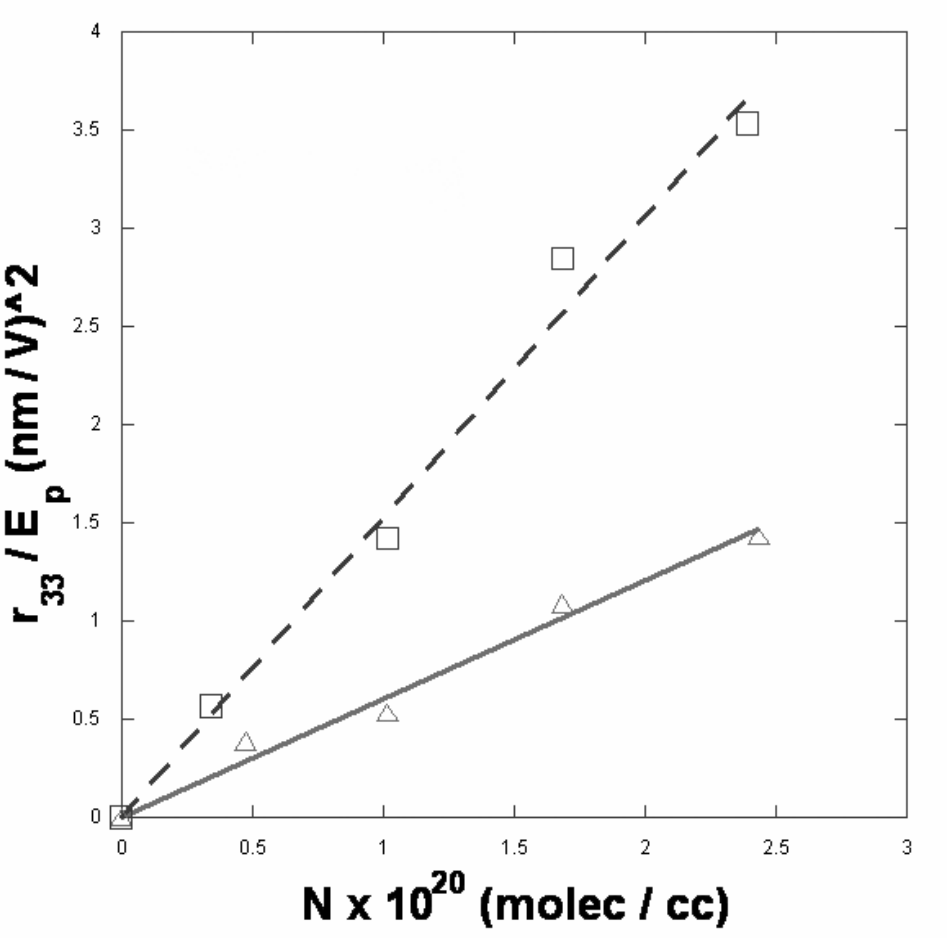

Fig. 14

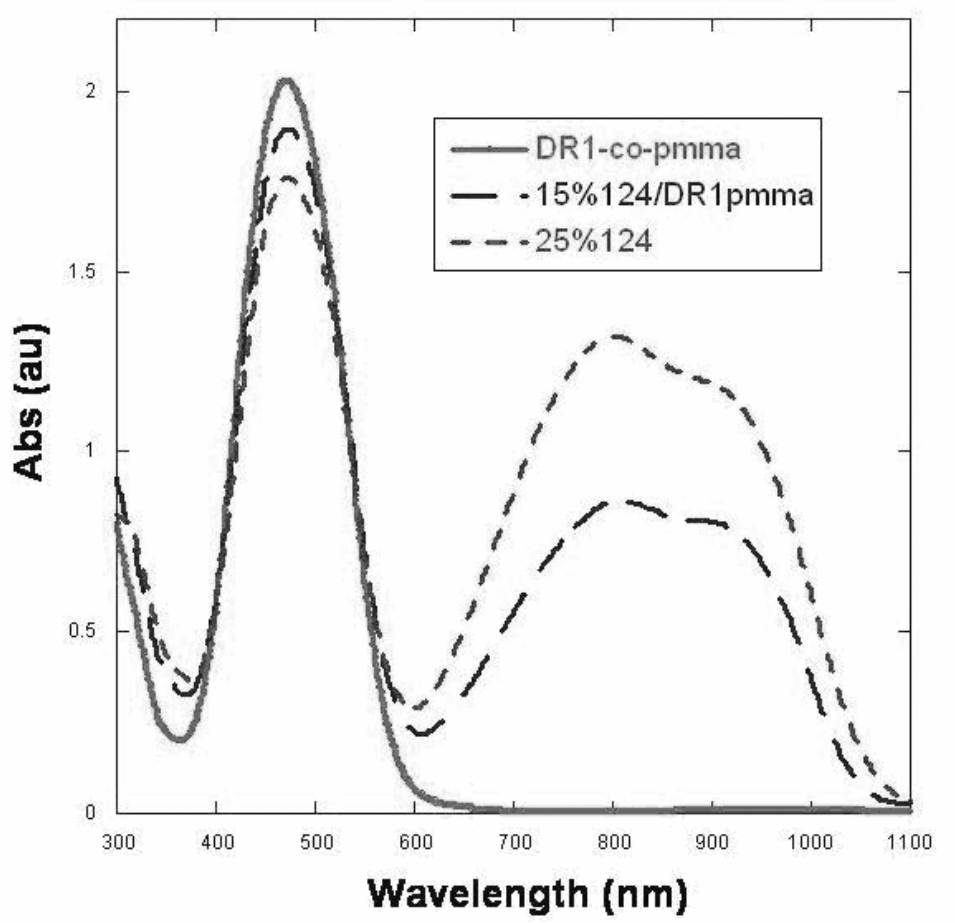
DR1-co-pmma
-15%124/DR1pmma
-25%124
Abs (au)
Wavelength (nm)
0
0.5
1
1.5
2
300
400
500
600
700
800
900
1000
1100

Fig. 15

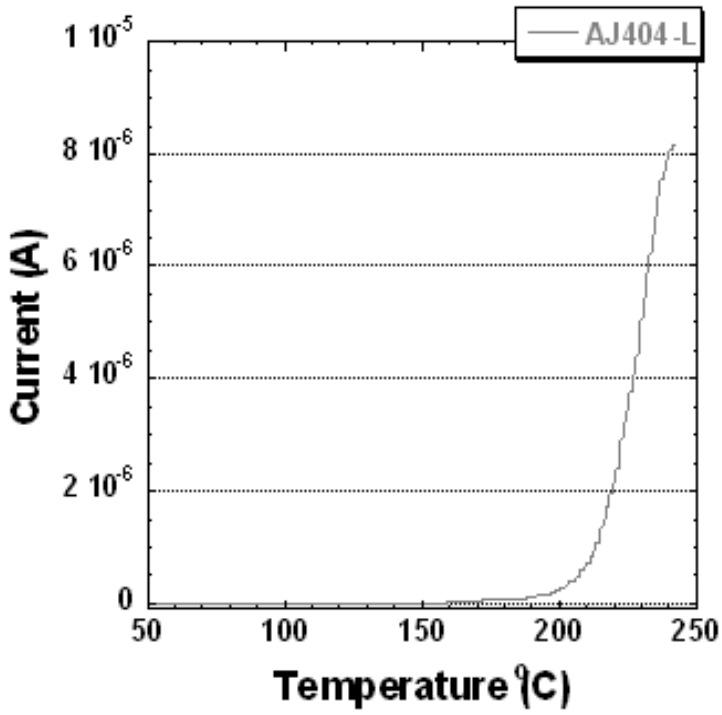
AJ404-L
1 10-5
8 10-6
6 10-6
4 10-6
2 10-6
0
Current (A)
50
100
150
200
250
Temperature (°C)

Fig 16

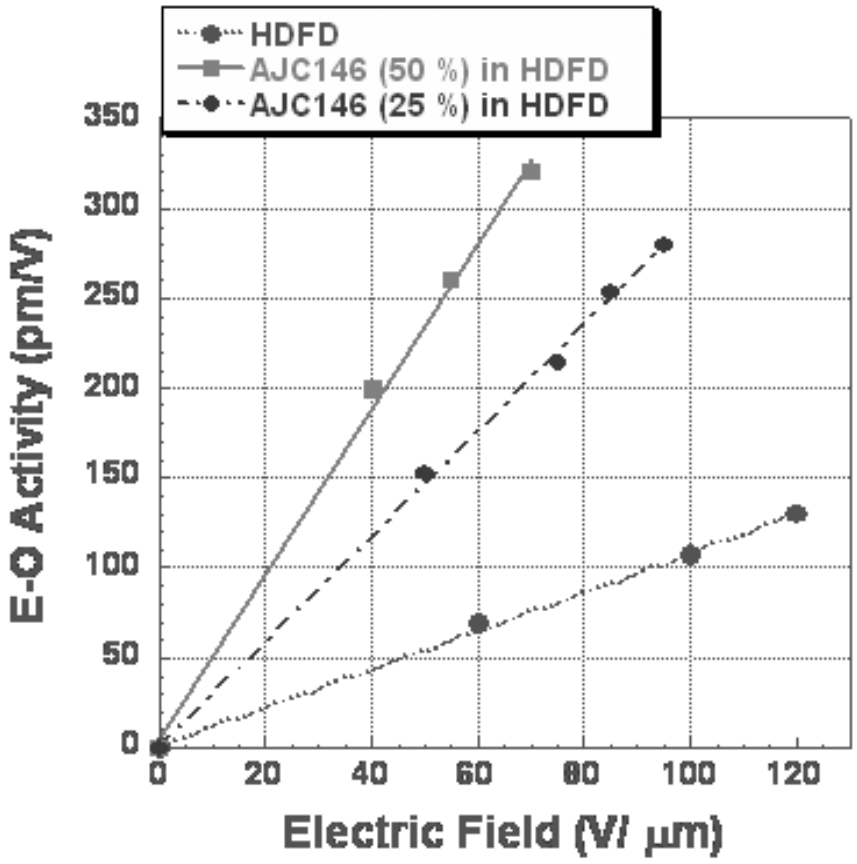
HDFD
AJC146 (50 %) in HDFD
AJC146 (25 %) in HDFD
E-O Activity (pm/V)
Electric Field (V/ μm)
0
50
100
150
200
250
300
350
0
20
40
60
80
100
120

Fig. 17

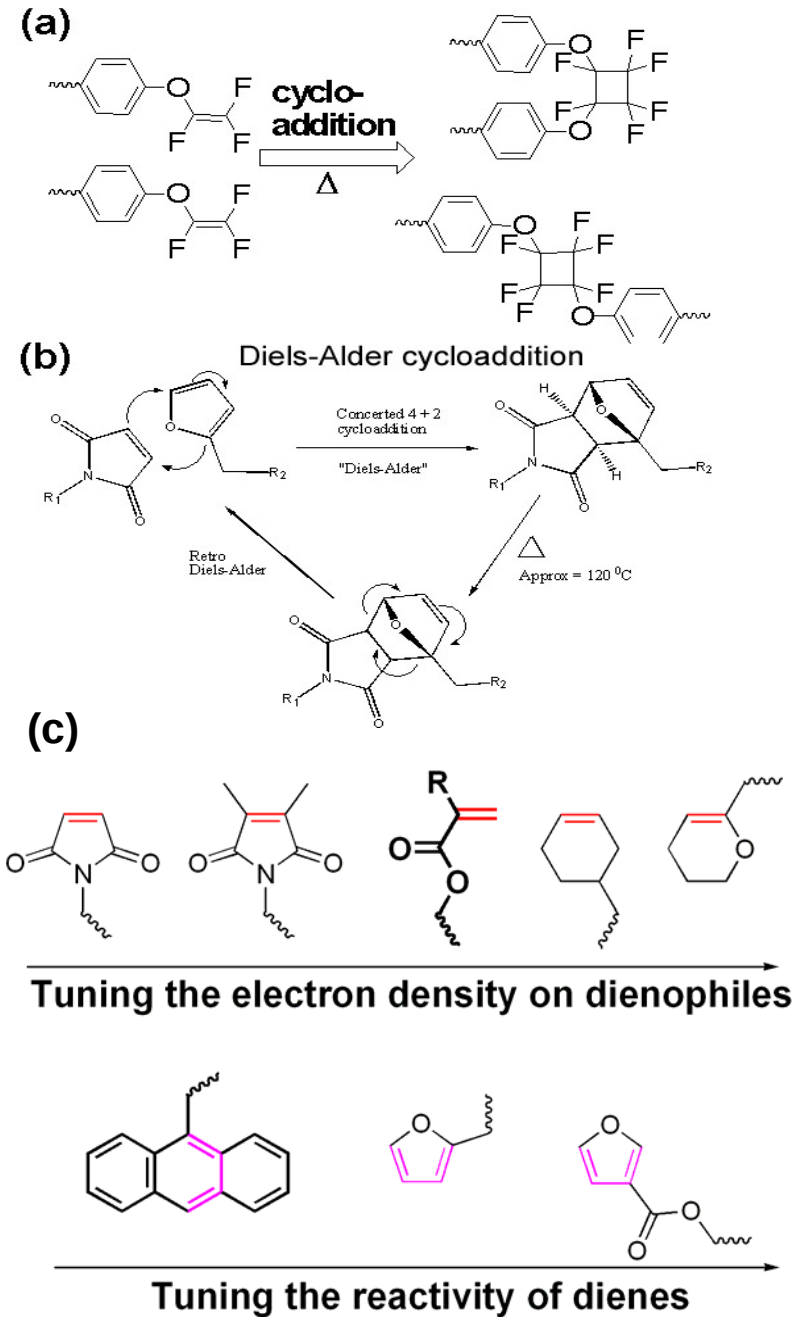
(a)
cyclo-
addition
Δ
(b)
Diels-Alder cycloaddition
Concerted 4 + 2
cycloaddition
"Diels-Alder"
Retro
Diels-Alder
Approx = 120 °C
(c)
Tuning the electron density on dienophiles
Tuning the reactivity of dienes

Fig. 18

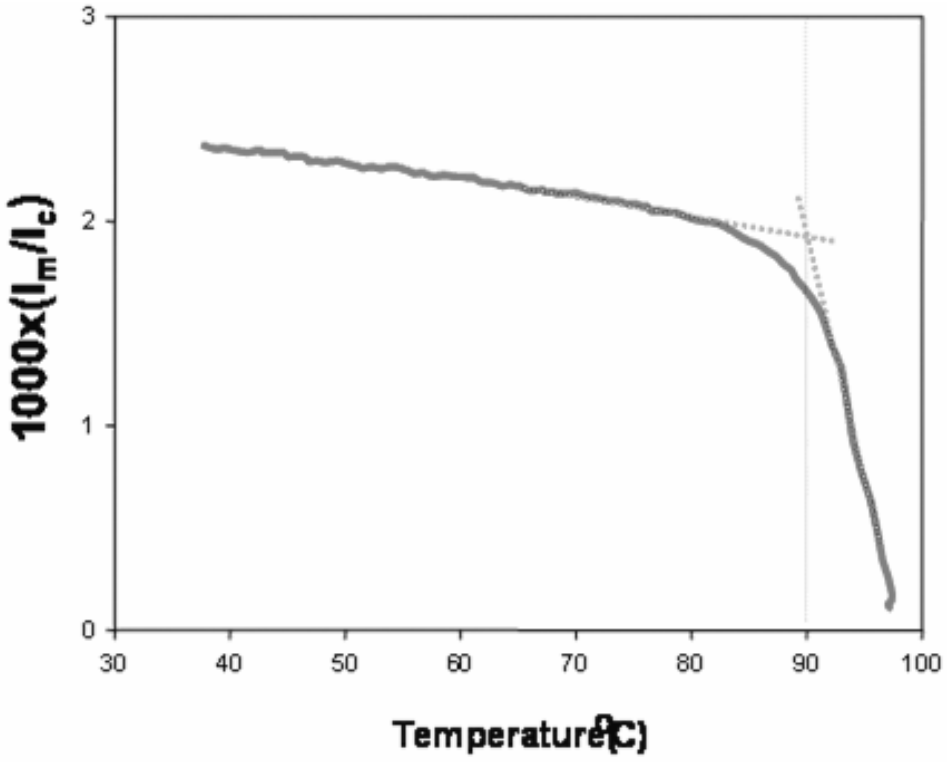

Fig. 19

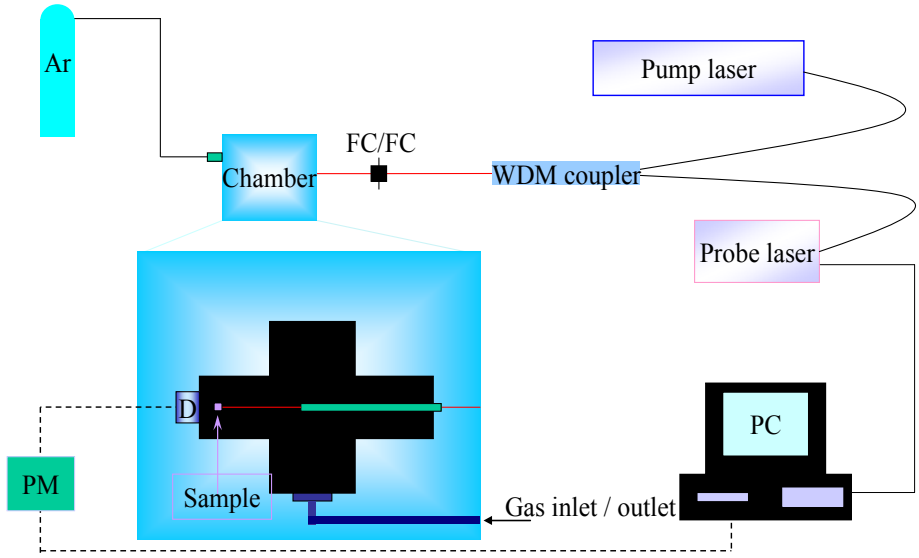
Ar
Pump laser
FC/FC
Chamber
WDM coupler
Probe laser
D
PC
PM
Sample
Gas inlet / outlet

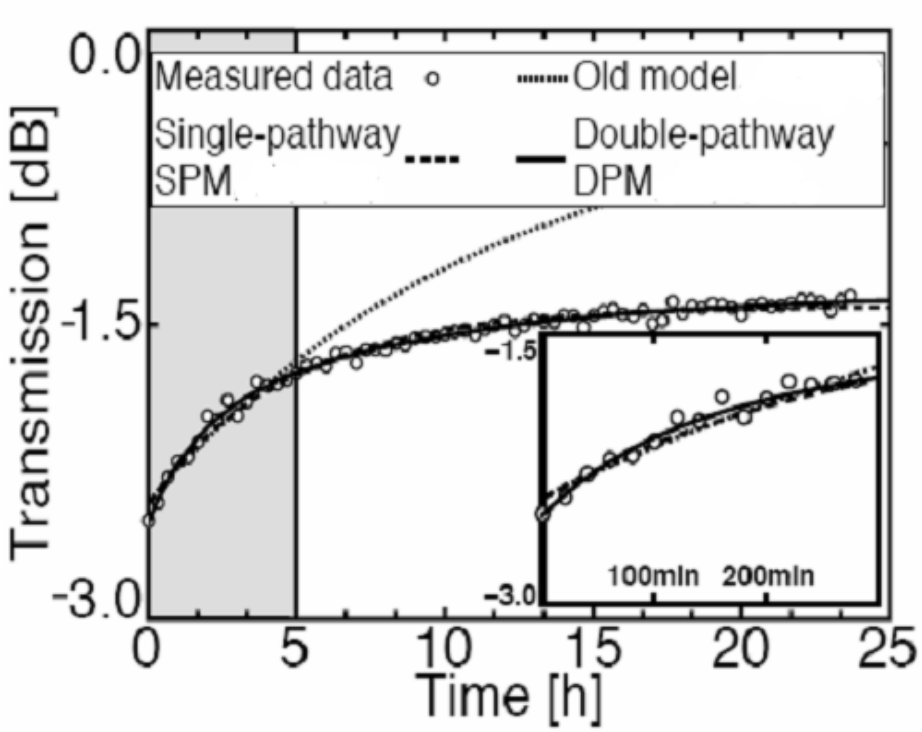
Measured data
Old model
Single-pathway SPM
Double-pathway DPM
Transmission [dB]
0.0
-1.5
-3.0
0
5
10
15
20
25
Time [h]
100min
200min

Fig. 20

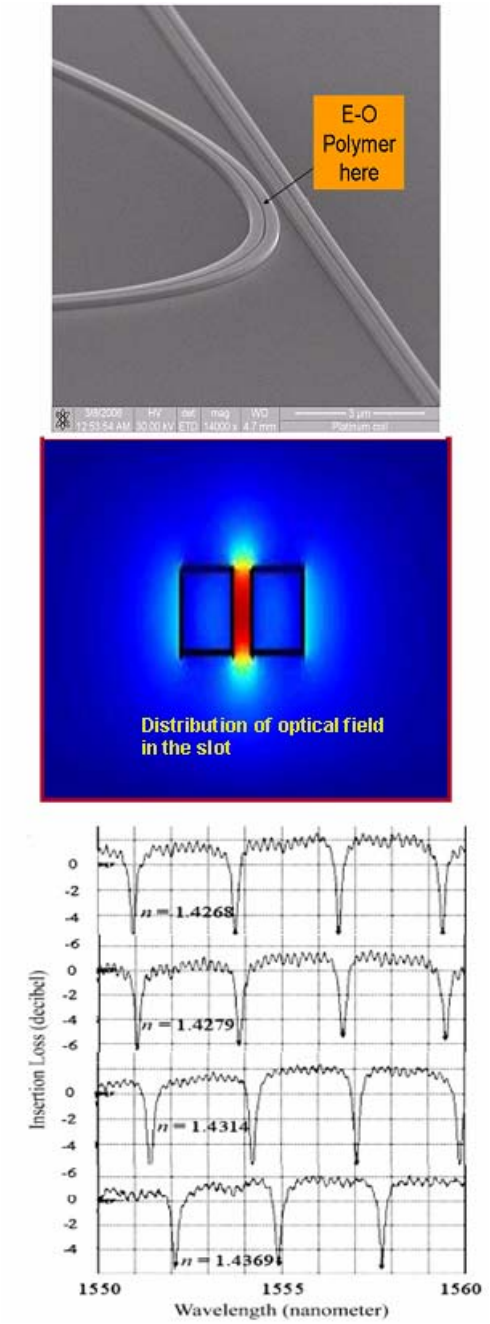
E-O
Polymer
here
Distribution of optical field
in the slot
n = 1.4268
n = 1.4279
n = 1.4314
n = 1.43691
Insertion Loss (decibel)
0
-2
-4
-6
1550
1555
1560
Wavelength (nanometer)

Table 1

EFISH data for EZ-FTC

Solvent	ε	λ_{max}/nm	$\mu\beta_{\omega}/10^{-69}$ SI (exp.)	$\mu\beta_0/10^{-44}$ esu(exp.)	$\mu\beta_0/10^{-44}$ esu(theory)
Dioxane	2.21	622	9291	3.41	4.9
Chloroform	4.81	675	27280	8.52	8.9

Table 2. Representative Photostability Data for FTC and CLD chromophore in APC

Sample	B/σ^a x10^{32} (m^{-2})	B/σ^b x10^{32} (m^{-2})	B/σ^c x10^{32} (m^{-2})
CLD-1 in APC	3.2 ± 0.6	0.18 ± 0.03	2.3 ± 0.6
CLD-1 + Bis(dithiobenzil)nickel in APC	8 ± 2	2.2 ± 0.7	19 ± 5
FTC in APC	7.2 ± 0.7	0.8 ± 0.3	8 ± 2
FTC + Bis(dithiobenzil)nickel in APC	66 ± 33	9 ± 10	165 ± 136